

The Attraction Effect in Perceptual Decision-Making: A Case of Dominance Asymmetry

Tapas Rath^{1,*}, Narayanan Srinivasan¹ and Nisheeth Srivastava¹

¹ Indian Institute of Technology Kanpur, Department of Cognitive Science, Kanpur, UP, India

Correspondence*:

Tapas Rath

tapasr@iitk.ac.in

2 ABSTRACT

3 The attraction effect (AE), or asymmetric dominance effect, occurs when the presence of a
4 clearly inferior decoy increases the choice of a target over a competitor. While robust in value-
5 based domains, findings with perceptual stimuli have been inconsistent, with some studies
6 even reporting reversals in triangular arrangements of stimuli. Across four experiments and
7 a reanalysis of prior data, we demonstrate that these inconsistencies are attributable to the
8 presence or absence of genuine item-wise dominance asymmetry.

9 Experiment 1 established that novel star-shaped stimuli reliably produced strong target–decoy
10 (TD) dominance over competitor–decoy (CD) dominance, whereas traditional rectangles showed
11 weaker but still positive asymmetry. Experiment 2 provided the first robust demonstration of a
12 positive AE with perceptual stimuli in a triangular layout using stars, while Experiment 3 showed
13 that rectangle stimuli, when presented in a triangular layout, produced an aggregate null rather
14 than a negative effect. Similarly, the reanalysis of data from a previous triplet experiment involving
15 bars stimuli pointed towards a null effect. Experiment 4 again linked inconsistent findings from
16 linear versus triangular alignment of triplet rectangles to the presence of asymmetric dominance,
17 while also demonstrating an interaction between the differential ease of comparison in pairs and
18 presentation format.

19 Together, these results demonstrate that AE is a robust phenomenon that emerges whenever
20 decoys create strong item-level dominance asymmetry. Apparent inconsistencies with perceptual
21 stimuli reflect stimulus-specific dominance structures. This work clarifies the boundary conditions
22 of the AE, reinforces its domain generality, and provides methodological guidance for future
23 research on context effects in perceptual decision-making.

24 **Keywords:** preference reversals, attraction effect, asymmetric dominance, perceptual, decoy

1 GENERAL INTRODUCTION

25 The principle of *Independence of Irrelevant Alternatives* (IIA) is foundational in rational choice theory,
26 stating that the relative odds of choosing between two alternatives should remain unchanged by the
27 introduction or removal of additional alternatives (Luce, 1957):

$$\frac{P(i|C)}{P(j|C)} = \frac{P(i|C')}{P(j|C')}$$

28 for options i, j in sets $C \subset C'$.

29 The *regularity* axiom is a related, but weaker, requirement that adding an alternative cannot increase the
30 probability of choosing any of the original options (Luce, 1977):

$$P(i|C') \leq P(i|C)$$

31 for any i in the original set.

32 Tversky's work in the 1970s empirically demonstrated violations of IIA—the “similarity effect” showed
33 that new, similar alternatives could alter relative choice odds between original items, challenging the basic
34 premises of deterministic choice theory (Tversky, 1972). In response to these findings, Luce observed that
35 regularity was the only rational choice axiom yet unviolated by data (Luce, 1977). This status changed
36 following the landmark study by Huber, Payne, and Puto (Huber et al., 1982), who showed that the
37 *attraction effect* violates regularity: the addition of a decoy can *increase* the choice probability of an
38 existing option. It is now recognized that regularity is a necessary but not sufficient condition for IIA: any
39 violation of regularity implies a violation of IIA, but IIA can be violated without a corresponding violation
40 of regularity.

41 The attraction effect (AE) or asymmetric dominance effect is a widely studied choice bias in decision-
42 making where the presence of a third option (the “decoy”: D) influences decision-makers to prefer one
43 of the original options (the “target”: T) over the other (the “competitor”: C). The phenomenon is both
44 practically and theoretically important. Practically, it serves as a behavioral nudge to influence consumers'
45 choices (Devine et al., 2025). Theoretically, as we discussed, it demonstrates a violation of the assumption
46 in rational choice theory: regularity, and hence IIA.

47 Over the past forty years, researchers have documented the attraction effect across various decision-
48 making contexts. For instance, choices under risk exhibit systematic shifts when a dominated alternative is
49 introduced (Farmer et al., 2017), and category-based inference similarly shows sensitivity to contextual
50 distractors (Trueblood, 2012; Choplin and Hummel, 2005). Preference for a target option also changes
51 in typical consumer goods settings (Huber et al., 1982; Noguchi and Stewart, 2014), as well as during
52 sequential motor planning tasks (Farmer et al., 2017). Beyond studies with adult humans, developmental
53 and comparative studies reveal that this context-dependent shift occurs in young children (Zhen and Yu,
54 2016), domestic cats (Scarpi, 2011), nonhuman primates (Parrish et al., 2015), various avian species
55 including hummingbirds (Bateson et al., 2003), amphibians such as frogs (Lea and Ryan, 2015), social
56 insects like honeybees (Shafir et al., 2002), and even in slime molds (Latty and Beekman, 2011).

57 Studies by Choplin and Hummel (2005) and Trueblood et al. (2013), which demonstrated attraction
58 effects even in the perceptual domain, became essential milestones in establishing the ubiquity of the effect
59 and challenging the possibility of cardinal representations of value in the brain (Vlaev et al., 2011). Cardinal
60 representations refer to models in which values are encoded on an absolute, context-independent scale,
61 allowing comparisons to be made based on fixed neural metrics. The presence of attraction effects in both
62 value-based and perceptual tasks indicates that the brain's encoding of magnitude is relative and context-
63 dependent, rather than strictly cardinal. Demonstrating these effects in perceptual judgments—where
64 attributes have clear physical units—provides strong evidence that context-dependent comparison processes
65 are fundamental and not restricted to economic or subjective value domains.

66 Despite its wide documentation across species and domains, recent years have seen a growing number
67 of studies reporting inconsistent, muted, or even reversed attraction effects (repulsion effect) (Frederick
68 et al., 2014; Yang and Lynn, 2014). However, Huber et al. (2014) identified several boundary conditions
69 that can constrain the effect: strong prior preferences between core options, difficulty detecting dominance,
70 individual variation in attribute weighting, and pronounced aversion to or preference for the decoy. They
71 argued that studies failing to meet one or more of these criteria unsurprisingly reported inconsistent effects.
72 Subsequent work has further highlighted such constraints. In the perceptual domain, Spektor et al. (2018,
73 2022) found reversed effects when stimuli were arranged in a triangular configuration, leading some to
74 question the domain generality of the attraction effect. Most notably, Trendl et al. (2021) rigorously tested
75 the attraction effect with naturalistic stimuli (movies), while satisfying all boundary conditions identified
76 by Huber et al. (2014). However, they observed a precisely zero effect, leading them to conclude that the
77 attraction effect may be limited to stylized experimental stimuli.

78 We suggest that these recent failures may reflect the violation of an additional, previously overlooked
79 boundary condition: the requirement that the decoy be truly asymmetrically dominated. We developed a

80 novel class of perceptual stimuli that affords clear and unambiguous asymmetric dominance (explained
81 below) and adopted a pairwise comparison framework commonly used in the choice literature (explained
82 next) to test whether restoring this relational structure reinstates the standard attraction effect.

83 1.1 Asymmetric Dominance of Decoy

84 The attraction effect, also known as the asymmetric dominance effect, occurs when the presence of a
85 clearly inferior decoy option increases the likelihood of choosing the target over the competitor (Huber
86 et al., 1982). Central to this phenomenon is the notion of *asymmetric dominance*—the structural relationship
87 between options in the choice set that differentiates targets, competitors, and decoys.

88 Historically, asymmetric dominance has been defined primarily in **attribute-based terms**, where a decoy
89 is considered asymmetrically dominated if it is inferior to the target on *every* attribute but is partially
90 dominated by (or equal to) the competitor on at least one attribute (Kaptein et al., 2016; Bhatia, 2013;
91 Zofák, 2016; Helgadóttir, 2015). For example, a decoy may be dominated by the target in both price and
92 quality but be better than or equal to the competitor in at least one attribute. This attribute-wise definition
93 of asymmetric dominance has guided much of the experimental literature in designing decoys.

94 However, the original conceptualization by Huber et al. (1982) adopts an **item-based** definition: an
95 alternative is asymmetrically dominated if it is dominated by one option in the choice set but not by
96 another. This perspective focuses on the overall dominance relationships between *whole options* rather than
97 isolating attribute-level comparisons. Importantly, this item-based asymmetry is broader and encapsulates
98 attribute-based definitions as a special case.

99 Formally, these definitions can be summarized as follows, where D_x and D_y denote decoy attribute
100 values, T_x and T_y target attribute values, and C_x and C_y competitor attribute values:

$$\text{Attribute-Based Asymmetric Dominance: } D_x \leq T_x, \quad D_y \leq T_y, \quad D_y \leq C_y, \quad D_x > C_x \quad (1)$$

$$\text{Item-Based Asymmetric Dominance: } P(T | TD) \gg 0.5, \quad P(C | CD) \approx 0.5 \quad (2)$$

101 where $P(X | XY)$ is the probability of choosing option X from binary pair XY , computable as choice
102 frequencies.

103 It should be noted, however, that the above formalizations concern only structural definitions of asymme-
104 try reflected in behavior, without any commitment to the underlying cognitive process. The distinction is
105 important because it separates structural boundary conditions about dominance asymmetry from assump-
106 tions about the cognitive comparison process. Our approach adopts the item-based definition of asymmetry
107 to remain as general as possible and focuses on measurable choice behavior without committing to specific
108 cognitive mechanisms (Banerjee et al., 2024b).

109 Figure 1 illustrates an example set of items located in a two-dimensional attribute space (x and y), where
110 the criterion value is given by the product of the attributes (i.e., $x \times y$). Here, item C represents a rectangle
111 with width = 5 units and height = 10 units, whereas item T represents a rectangle with width = 10 units
112 and height = 5 units. Assuming that the two rectangles are perceived as equivalent in area (each having 50
113 square units), a decoy is an item that is inferior to the target in one or both attributes and thereby favors the
114 target. If the decoy is inferior to the target in the target's strongest attribute, it is called a frequency decoy
115 (D_F); if it is inferior to the target in the target's weakest attribute, it is called a range decoy (D_R). If the
116 decoy is inferior to the target in both attributes, it is called a range-frequency decoy (D_{RF}) (Huber et al.,
117 1982). For simplicity, we consider here D_R , which corresponds to a rectangle with an area of 40 square
118 units.

119 Imagine we ask subjects to rank-order the items along one attribute dimension at a time. Irrespective of
120 whether they do an ordinal comparison of two or three items at a time, the decoy in our example will be
121 asymmetrically dominated according to the attribute-based definition, since it does not surpass the target
122 on either attribute but is at least as good as, or better than, the competitor on one attribute dimension.
123 In contrast, if we present pairs of items at a time and ask subjects to make choices based on the overall
124 criterion values, and they integrate the two attributes into a common currency (here, area), the same decoy

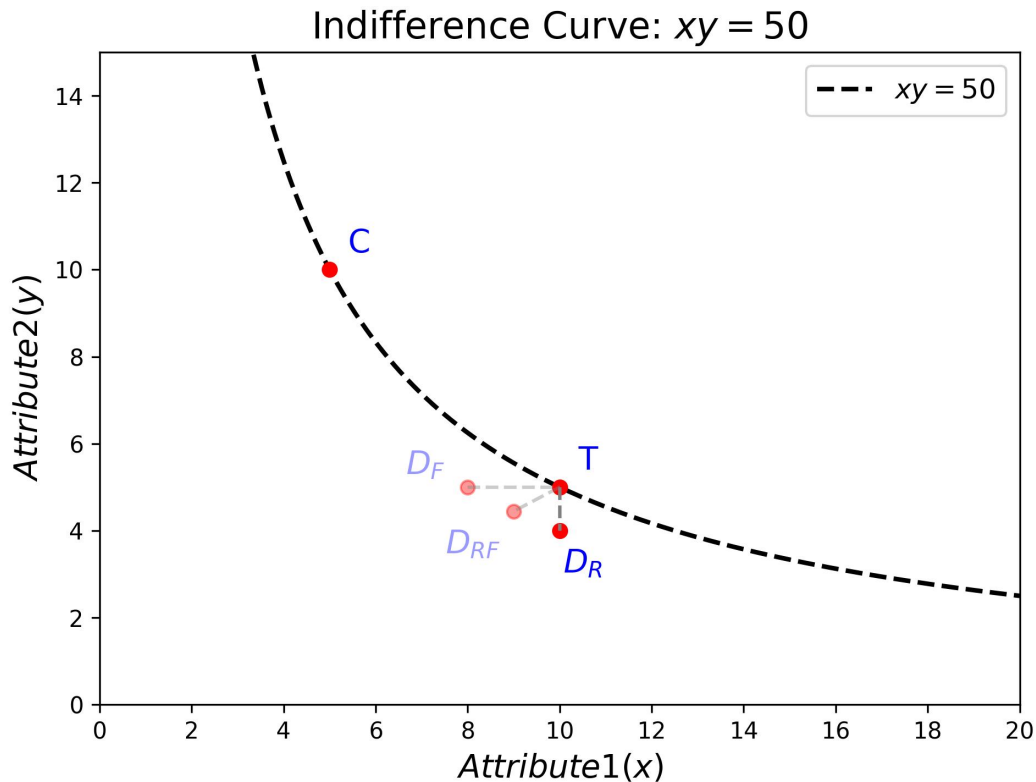


Figure 1. Example of asymmetric dominance in a two-attribute space. The dashed curve shows the indifference curve ($xy = 50$). Items *C* and *T* lie on the curve (area = 50). Three possible decoys are shown: D_F (frequency decoy), D_R (range decoy), and D_{RF} (range-frequency decoy).

125 will no longer be asymmetrically dominated (the item-based definition). Instead, it will be symmetrically
 126 dominated by both the target and the competitor (each with an area of 50 compared to the decoy's 40).

127 1.2 Pairwise Comparisons

128 Sequential sampling models have provided a rich framework for understanding multi-alternative, multi-
 129 attribute choice by viewing decision making as a process of repeated comparisons among options and
 130 attributes, with attention shifting to compare and evaluate subsets of options throughout the deliberation
 131 process (Roe et al., 2001; Usher and McClelland, 2004). Prominent models of choice (Russo and Doshier,
 132 1983; Wollschläger and Diederich, 2012; Kornienko, 2013; Trueblood et al., 2014; Ronayne and Brown,
 133 2017; Noguchi and Stewart, 2018; Evans et al., 2021) assume that this subset is a pair—pairwise compar-
 134 isons are at the heart of these models. Eye-tracking studies (Noguchi and Stewart, 2014) also suggest that
 135 alternatives are compared in pairs, often along a single attribute dimension.

136 We primarily draw inspiration for our asymmetric dominance thesis from the stochastic ordinal compari-
 137 son model introduced by Srivastava and Schrater (2015). Their framework formalizes decision-making as
 138 a Bayesian inference problem, where the relative desirability of an option is computed from past choice
 139 histories across varying contexts. In this setting, the model infers probabilistic desirabilities by considering
 140 the likelihood that an item would be chosen in each observed subset of options, with attentional weights
 141 operationalized as the probability of encountering each context. Rather than assigning exogenous utility
 142 values, the model learns from observed pairwise choice outcomes and histories to update its beliefs about
 143 the desirability of each item, yielding measurable choice probabilities that reflect context-sensitive and
 144 history-dependent preference structures.

145 For a simpler illustration, we present a non-stochastic version of the ordinal pairwise comparison model,
 146 formally defined as follows. Consider a set of alternatives $\{A_1, A_2, \dots, A_m\}$. Each alternative is evaluated

147 by comparing it pairwise with every other alternative. For any comparison between A_i and A_j ($i \neq j$), the
 148 model assigns to A_i a score $V_i(A_i, A_j)$, where $V_i(A_i, A_j) = 1$ if A_i wins, $V_i(A_i, A_j) = 0$ if A_j wins or
 149 there is a tie. The total evidence for A_i is then

$$V_i = \sum_{j \neq i} V_i(A_i, A_j),$$

150 and the selected alternative is

$$A^* = \arg \max_i V_i \quad (\text{the alternative with highest } V_i).$$

151 To accommodate cases in which some pairs are compared more frequently or are given greater attentional
 152 weight, we introduce non-negative weights n_{ij} for each ordered pair (A_i, A_j) , yielding the generalized
 153 evidence function

$$V_i = \sum_{j \neq i} n_{ij} V_i(A_i, A_j).$$

154 Table 1 presents the simplest case with $n_{ij} = 1$ for all $i \neq j$, in which each pair is compared once. This
 155 highlights how cumulative pairwise victories can capture asymmetric dominance and thereby influence
 156 the final choice. This formulation is descriptive: it specifies how aggregate outcomes arise through the
 157 sequential, weighted aggregation of pairwise wins, without committing to any particular psychological
 158 or computational process that generates the individual scores $V_i(A_i, A_j)$. Each computation may involve
 159 comparisons along single attribute dimensions or holistic evaluations, depending on the structure and
 160 commensurability of the attributes. By leaving the basis of comparison unspecified, the model remains
 161 general and applicable across contexts. Moreover, the framework allows direct experimental manipulation of
 162 the attentional weights n_{ij} , while keeping the aggregation rule itself agnostic to the underlying comparison
 163 process.

Table 1. Pairwise “votes” for ordinal comparison scenarios: (A) AE occurs; (B) No AE.

	Pairwise Contest	Winner	Points to T	Points to C
(A) AE	T vs. D	T	+1	0
	T vs. C	Tie	0	0
	C vs. D	D or Tie	0	0
	Total		1	0
(B) No AE	T vs. D	T	+1	0
	T vs. C	Tie	0	0
	C vs. D	C	0	+1
	Total		1	1

164 Other influential models in the literature provide complementary perspectives on pairwise comparison and
 165 attention. [Noguchi and Stewart \(2018\)](#) propose the Multialternative Decision by Sampling (MDbS) model,
 166 where decision makers randomly sample attribute-option pairs and make ordinal judgments. Process-tracing
 167 data indicate that gaze shifts between pairs drive context effects through differences in winning frequencies.
 168 MDbS emphasizes attribute-wise ordinal sampling but does not explicitly model asymmetric dominance at
 169 the item level.

170 The Attribute Commensurability and Context Effects (ACE) model, proposed by [Hayes et al. \(2024\)](#)
 171 highlights how the comparability of attribute scales influences attentional allocation and, consequently,
 172 context effects. Incommensurable attributes produce salient, discriminable comparisons, resulting in robust
 173 context effects, whereas commensurable scales lead to holistic processing and attenuated effects. This
 174 work formalizes an important link between attribute presentation, attention, and context effects, though
 175 asymmetric dominance is operationalized indirectly via attention modulation.

176 [Cataldo and Cohen \(2019\)](#) offer a flexible comparison-process framework that explains attraction,
177 compromise, and similarity effects by how attentional focus shifts between dimension-level and alternative-
178 level comparisons based on presentation format. Their account emphasizes how stimulus format affects
179 cognitive comparison strategy, but does not treat asymmetric dominance as a mandatory structural condition.

180 Finally, [Trueblood et al. \(2022\)](#) introduce an attentional dynamics model that captures both attraction and
181 repulsion effects through flexible allocation of attention in multi-attribute choice. Their model suggests that
182 repulsion effects emerge when attention disproportionately focuses on dissimilar alternatives, reversing
183 expected dominance patterns. This highlights the dynamic nature of attention but does not explicitly embed
184 asymmetric dominance as a fixed principle.

185 Together, these models underscore the importance of pairwise comparisons and attentional weighting
186 in explaining context effects. The [Srivastava and Schrater \(2015\)](#) model uniquely integrates asymmetric
187 dominance as a core component while allowing attention to operate independently, providing the theoretical
188 foundation for our asymmetric dominance thesis. Other models may be extended to include explicit
189 dominance asymmetry, which remains an avenue for future work.

190 1.3 Overview of Experiments

191 The current investigation systematically explores the role of item-level asymmetric dominance and
192 attentional modulation in driving the attraction effect across four experiments.

193 Experiment 1 serves as a diagnostic test to establish dominance asymmetry in binary (pairwise)
194 comparisons. We introduce a novel class of star-shaped stimuli designed to reliably produce robust
195 dominance asymmetry, comparing their performance against traditional rectangular stimuli known to
196 produce inconsistent or reversed attraction effects ([Spektor et al., 2018](#)).

197 Building on these pairwise dominance findings, Experiment 2 tests whether the star stimuli elicit a classic
198 attraction effect in a triplet choice context, assuming the same underlying process in both pair and triplet
199 choice context.

200 Experiments 3 and 4 address a long-standing puzzle in the perceptual literature: why traditional rectangu-
201 lar stimuli produce positive attraction effects when arranged linearly but reversed effects when arranged
202 in triangular configurations. Experiment 3 investigates this effect through a controlled replication, while
203 Experiment 4 systematically manipulates spatial layout to test attentional mechanisms implicated in
204 modulating evidence accumulation.

205 Collectively, these studies provide a comprehensive empirical test of the boundary condition that asym-
206 metric dominance of the decoy, coupled with attentional sampling processes, governs the presence and
207 magnitude of attraction effects in perceptual choice.

2 EXPERIMENT 1

208 2.1 Introduction

209 In the pre-registered within-subjects experiment 1, we used two independent variables—stimulus type
210 (rectangle vs. star) and comparison pair (CD vs. TD). We predicted a significant interaction effect on the
211 dependent variables of accuracy and reaction times. In addition, we collected perceived difficulty ratings of
212 choice (exploratory) when alternatives were compared in pairs.

213 2.2 Method

214 2.2.1 Participants

215 Sixty-seven (15 female) university students with normal or corrected-to-normal vision (M: 21.57 years,
216 SD: 2.88, range: 17-31), participated in the study.

217 2.2.2 Apparatus and Stimuli

218 The experiment was designed using JavaScript and conducted on laboratory computers with screen
219 resolutions of 1920 px × 1080 px and a screen size of 24 inches (16:9). Stimuli were presented in pairs

220 (target-decoy pairs and competitor-decoy pairs), and consisted of two types of shapes: rectangles and
221 star-like shapes.

222 In each trial, the stimuli consisted of two horizontally aligned black-colored shapes on a white background.
223 The two stimuli were positioned horizontally around the screen center at 30% and 70% of the total screen
224 width ($x = 576$ px and $x = 1344$ px, respectively), separated by 768 px (≈ 21.3 cm; $\approx 20.1^\circ$ of visual
225 angle at a 60 cm viewing distance). The vertical positions of the stimuli were jittered across trials. The
226 stimulus pair for each trial was derived from the respective set of triplets, which in turn were created in steps
227 from the core stimuli. The term core stimuli refers to the two base stimuli forming the primary comparison
228 set in each trial—the Target (T) and Competitor (C). These rectangular shapes were pre-generated and
229 matched on the relevant decision criterion (equal area) to ensure baseline equivalence before constructing
230 decoy variations. Decoy stimuli (D) were subsequently derived from these core shapes by systematically
231 adjusting one or both dimensions. In each trial, either a target-decoy pair or a competitor-decoy pair was
232 displayed.

233 2.2.2.1 Rectangle Stimulus

234 To generate the rectangle-based stimuli, we first created a set of 6 random rectangles (the “W” set, wide)
235 by sampling from a bivariate normal distribution (mean height: 170 px, mean width: 250 px; standard
236 deviation: 25 px for each attribute, no correlation), following Spektor et al. (2018). To create matched but
237 vertically oriented rectangles (the “N” set, narrow), the width and height of the W set were swapped for
238 each pair, preserving area but altering orientation. This resulted in 6 core pairs, each consisting of a wide
239 (W) and a narrow (N) rectangle.

240 For each of the 6 core pairs, we randomly assigned one of three trial types (range, frequency, range-
241 frequency) (Huber et al., 1982), with each trial type appearing twice across the 6 pairs. Following the
242 triplet-triplet design by Wedell (1991), for every pair, two sets of triplets were generated: (1) with W as
243 the target (T) and N as competitor (C), and (2) with N as the target and W as competitor. For each triplet,
244 a decoy rectangle (D) was constructed based on trial type manipulation rules (by reducing width and/or
245 height by 10 to 25 px relative to the target rectangle, according to the assigned trial type).

246 This procedure yielded 12 triplets (6 W-target, 6 N-target), each consisting of a T, C, and D rectangle.
247 For each triplet, two experimental trials were constructed by presenting either the Target-Decoy (TD) pair
248 or the Competitor-Decoy (CD) pair. Thus, the rectangle stimulus set resulted in a total of 24 experimental
249 trials per participant.

250 Quantitatively, the resultant target-decoy distance—measured as the relative difference in *criterion values*
251 considering both attributes—had a mean of 11.36% (SD = 2.17%) and ranged from 8.43%–14.71%. The
252 distribution was approximately symmetrical without strong skewness.

253 2.2.2.2 Star Stimulus

254 A parallel procedure was followed for star-shaped stimuli. Each star-like shape was derived from a base
255 rectangle, with four distinct sections removed. These sections consisted of two pairs of inward-facing
256 isosceles triangles, where the bases of the triangles were equal to and touched the four sides of the rectangle,
257 resulting in a star-like shape. Figure 3, panels A and B, display two sample trials.

258 The shape characteristics were determined by two key parameters: the base rectangle’s width and the
259 height of the removed triangles. Specifically, for the first out of the two sets of core stimuli, the mean
260 rectangle width (μ_{w_1}) was set to 180 px, while the mean triangle height (μ_{d_1}) was set to 40 px. The
261 respective variances were 30 px ($\sigma_{w_1}^2$) and 40 px ($\sigma_{d_1}^2$), with no correlation between the two.

262 Additionally, the height H_1 for the shape was determined by adding a random adjustment to the width.
263 This adjustment was drawn from a normal distribution with a mean of 20 px and a standard deviation of 5
264 px. The value of H_2 , representing the second height, was set equal to H_1 .

265 The participants were instructed that the shapes represented objects drawn with sand, and their task was
266 to identify which of the given shapes would require the least amount of extra colored sand to be extended
267 into a perfect square. Of the two core shapes, one had a wider base rectangle and a larger removed triangle
268 height, while the other had a narrower base rectangle and a proportionally smaller removed triangle height.
269 For simplicity, we refer to the wider shape as “W” (wide) and the narrower shape as “N” (narrow).

270 To generate the stimuli, the W shapes were created first using the width and height distributions mentioned
271 above. Then, ensuring that both W and N shapes required the same amount of extra area to form a perfect
272 square, the N shapes were derived. As with rectangles, 6 core pairs of W/N stars formed the basis of
273 the stimulus set. Each core pair was randomly assigned one of three trial types (range, frequency, range-
274 frequency), such that all types appeared twice. For each pair, both possible target-competitor arrangements
275 (W as target, N as target) were used. Corresponding decoy stars were created by manipulating the base
276 rectangle's width (reduced by 8–15 px) and the height of the removed triangles (increased by 4–7 px)
277 relative to the target, according to the assigned trial type. Thus, there were 12 triplets (6 W-target, 6
278 N-target), each producing two experimental trials (TD and CD). This resulted in 24 experimental star trials
279 per participant.

280 The target-decoy distance—measured as the relative difference in *criterion values* considering both
281 attributes—had a mean of 13.97% (SD = 2.14%) and ranged from 10.53% to 16.91%. The distribution was
282 approximately symmetrical without strong skewness.

283 Additionally, 12 catch trials were included throughout the experiment. In these trials, participants always
284 received the instruction: “Choose the shape that requires the least amount of extra coloured sand to make
285 it a perfect square.”—the same instruction as for star trials. Catch trials presented vertically oriented
286 rectangles pairs designed so that one option clearly required less extra sand to complete into a square than
287 the other, varying in only one attribute (width for rectangles).

288 To summarize, each participant completed 24 rectangle-based trials, 24 star-based trials, and 12 catch
289 trials, for a total of 60 trials. For rectangle stimuli, the criterion value was defined as the area (width ×
290 height). For star stimuli, the criterion value was the area of additional 'sand' required to complete the shape
291 into a perfect square, calculated using the geometric parameters of the base rectangle and the removed
292 triangles. The OSF repository contains the exact stimulus set. In the *Supplementary Material section 1*, we
293 present further details on the star stimuli creation with the full formula for criterion value matching.

294 Although the rectangle and star stimuli involved different surface attributes (rectangles: width and height;
295 stars: base width and height of the removed triangular section) and corresponded to different judgment
296 tasks (estimating overall area versus estimating sand required to complete a square), in both cases, stimulus
297 variation was systematically governed by two orthogonal attributes. Importantly, decoy manipulations were
298 constructed within the same underlying attribute framework, ensuring consistency in the experimental
299 implementation of the attraction effect across the two stimulus types.

300 2.2.3 Design

301 The experimental conditions were defined by two independent variables: (1) Stimulus Type (rectangle
302 vs. star), and (2) Comparison Pair (Target-Decoy [TD] vs. Competitor-Decoy [CD]). In a within-subjects
303 design, each participant experienced all four combinations of these variables: (1) Rectangle, CD, (2)
304 Rectangle, TD, (3) Star, CD, and (4) Star, TD.

305 The trials were presented using block randomization to ensure balanced exposure to all conditions. The
306 experiment consisted of 12 blocks, each containing one trial per condition. Each condition was presented
307 12 times, resulting in 48 experimental trials. The Fisher-Yates algorithm was applied to randomize the order
308 of conditions within each block, ensuring that the sequence of trials was unpredictable while maintaining
309 balance. Additionally, 12 catch trials were included as exclusion criteria and were randomly interspersed
310 throughout the experiment. The catch trials were distributed across the trial sequence using the same
311 randomization method, ensuring a unique and unbiased presentation for all participants.

312 Each trial comprised a choice response phase followed by a rating task, with no time constraints imposed.
313 The number of trials per participant was selected to balance robust data collection with participant comfort.
314 Our design maximized data quality and engagement while minimizing fatigue, in light of the absence
315 of imposed time constraints and the inclusion of additional rating tasks in each trial. Moreover, recent
316 simulation-based evidence (Miller, 2024) demonstrated that increasing participant sample size typically
317 contributes more to statistical power than a dramatic increase in trial numbers, especially when longer
318 experimental durations risk inducing fatigue or noncompliance. Reduced trial load thereby supports better
319 data reliability and sustained task engagement in within-subject perceptual and decision-making paradigms.
320 Additionally, stimulus randomization and block balancing procedures ensured full counterbalancing of all
321 relevant conditions, supporting robust statistical inference despite a modest number of trials per participant.

322 2.2.4 Procedure

323 At the beginning of each trial, a fixation cross was presented for 500 ms. This was immediately followed
324 by the stimulus display, which remained on the screen until the participant responded via key press—there
325 was no time limit imposed for the choice response. Upon making a selection, a rating task appeared, which
326 similarly remained visible until a key press response was recorded. There was no time restriction for ratings.
327 After each trial, the next fixation cross was presented for 500 ms before the onset of the following trial.

328 For rectangle trials, participants were instructed to select the rectangle with the largest area. For trials
329 with star-like shapes, they were instructed to choose the shape requiring the least amount of additional
330 colored sand to extend it into a perfect square. Participants selected the alternative in each trial using the
331 left or right arrow keys. Following their decision, using number keys 1-7, they rated the difficulty of their
332 choice on a 7-point Likert scale, where one represented "extremely easy" and seven represented "extremely
333 difficult."

334 Before the main experiment, each participant completed a feedback-based practice session which involved
335 only star stimuli. These practice trials ensured comprehension of the more complex stimulus evaluation
336 instructions. No separate practice was required for the rectangular stimuli, as participants readily understood
337 and performed this task during pilot testing. In the practice session, the participants were presented with 10
338 pairs of star shapes in random order. In five trials, the W stimulus was the expected answer, and in five trials,
339 the N stimulus was the expected answer. Participants could click on each black shape to transform it into
340 a perfect square, with the extra-filled portion highlighted in red. When a shape was clicked, a numerical
341 value representing the extra sand required (e.g., 21,458 units) appeared below the shape in an arbitrary
342 unit of measurement. The practice session was to ensure that participants understood the task instructions,
343 especially for the star task.

344 2.3 Results

345 Out of a total of 67 participants, we excluded data from 6 participants because their performance was
346 lower than 0.8 in the catch trials, where in each trial, there was clearly one best option out of the two.
347 Additionally, we excluded a total of 119 individual trials (4.06%) that were either too fast (<100 ms) or
348 too slow (>20,000 ms).

349 We performed repeated measures ANOVAs on accuracy, reaction time, and perceived difficulty ratings.
350 The interaction effects of *Stimulus Type* (Star vs. Rectangle) \times *Comparison Pair* (CD vs. TD) on all three
351 were significant. ANOVA results are in Table 2. Interaction plots are shown in Figure 2. The main effects of
352 the pair were significant for difficulty rating, accuracy, and RT. On average, the CD pair was rated as more
353 difficult than the TD pair, and performance (both accuracy and RT) was better for the TD pair than the CD
354 pair. Similarly, the main effects of stimulus type were also significant for accuracy and RT. Performance for
355 rectangular stimuli (both RT and accuracy) was better compared to star stimuli. However, considering both
356 the stimulus type and the comparison pair interaction, the pattern of results diverged between the stated
357 difficulty and the revealed difficulty (as measured by accuracy), as well as RT.

358 In the post hoc analysis, the accuracy difference between the two pairs was significant for the star stimuli
359 ($t(60) = 7.079$, $p < 0.001$, Cohen's $d = 1.016$, mean difference = 0.180, SD = 0.199). In contrast, the
360 TD CD accuracy difference for rectangle stimuli, while still significant, was notably smaller ($t(60) =$
361 5.092 , $p < 0.001$, Cohen's $d = 0.576$, mean difference = 0.085, SD = 0.130). Moreover, a pairwise t -test
362 between the delta accuracies (TD-CD) for the two stimulus types (star vs. rectangle) revealed a significant
363 difference, $t(60) = 3.132$, $p = 0.003$, Cohen's $d = 0.567$.

364 To ensure that the observed differences between stimulus types were not driven by variability in the
365 distribution of %Target-Decey distances (TD_dist%), we conducted a supplementary sensitivity analysis
366 that included only trials where the TD_dist% ranges overlapped for both rectangular and star stimuli.
367 The results of this analysis closely mirrored those derived from the full dataset, confirming that the
368 reported effects reflect genuine stimulus-type differences rather than artifacts of distributional variation
369 (see *Supplementary Material, Section 2*, for details). Additionally, robustness checks that varied participant
370 exclusion thresholds and trial-level RT cutoffs (Supplementary Table S5) revealed that the observed pattern
371 of results for accuracy remained stable across all tested criteria.

Table 2. Repeated measures ANOVA results for accuracy, reaction time, and difficulty rating. Each row reports the F value, p value, and partial eta squared (η_p^2) for the corresponding main effect or interaction.

Factor	$F(1, 60)$	p	η_p^2
Accuracy			
Stimulus type	11.06	.002	.16
Pair	75.82	< .001	.56
Stimulus type \times Pair	9.81	.003	.14
Reaction Time			
Stimulus type	27.08	< .001	.31
Pair	9.62	.003	.14
Stimulus type \times Pair	4.47	.039	.07
Difficulty Rating			
Stimulus type	2.50	.119	.04
Pair	22.82	< .001	.28
Stimulus type \times Pair	8.77	.004	.13

372 2.4 Discussion

373 Using accuracy as a proxy for decoy's dominance, the results support our hypothesis regarding the
 374 asymmetry of dominance, at least in the pairwise comparisons. The strong main effect of pair in the
 375 accuracy results reveals a differential accessibility of dominance relations between TD and CD pairs. This
 376 likely arises because the Target and Decoy (T and D) are close in attribute space, affording easier ordinal
 377 comparisons—often directly along a single attribute dimension. In contrast, the Competitor and Decoy
 378 (C and D) are placed farther apart in the attribute space, such that each alternative tends to be superior on
 379 different attributes: one is stronger on one attribute, while the other excels on another. This configuration
 380 reduces the ease of establishing clear ordinal dominance in CD pairs, requiring attention to trade-offs or
 381 joint evaluation across attributes.

382 The interaction effect in the accuracy results suggests that the decoy's dominance asymmetry was strong,
 383 though not ideal, for star stimuli but less pronounced for rectangle stimuli. To rule out the possibility that
 384 these results were influenced by a baseline preference bias for either wide (W) or narrow (N) core options,
 385 we fit a linear mixed-effects model including target type and its interaction with pair type. The interaction
 386 was not significant ($p = .54$), confirming that the dominance asymmetry was robust across both W and N
 387 targets (see the Supplementary Material section 3 for full details).

388 Surprisingly, for self-reported difficulty and RT, there was a difference between CD and TD only with
 389 rectangular stimuli. It is not clear why the less accurate star stimuli do not show a significant difference in
 390 RT and perceived difficulty between the CD and TD pairs. One possible explanation is that the star stimuli,
 391 by virtue of their more complex and novel geometry, were generally perceived to be at a higher level of
 392 task difficulty that reduced participants' sensitivity to subtle pairwise differences. This increased overall
 393 challenge may have led to greater variance both within and across participants, thereby masking any RT
 394 or perceived difficulty effects that would otherwise mirror the strong asymmetry observed in accuracy.
 395 Alternatively, the star task may have encouraged a more deliberative or strategy-driven mode of processing,
 396 such that participants did not rely on "fast" ease-of-comparison cues to the same extent as with familiar
 397 rectangles. This difference in cognitive approach could dampen RT and subjective difficulty differences,
 398 even as underlying choice asymmetries remain robust. Future work could probe these possibilities by using
 399 eye-tracking or confidence ratings to directly compare processing dynamics across stimulus types.

400 Note that while the star stimuli produced robust asymmetric dominance, with participants reliably
 401 preferring the target over the decoy in TD pairs but not showing similar choice in CD pairs, rectangles
 402 also showed significant, though weaker, asymmetry. Thus, although stars provide a stronger diagnostic of
 403 dominance asymmetry, even rectangles cannot be considered entirely free of item-level asymmetry.

404 Having established that star stimuli yield a particularly clear dominance structure, we next asked whether
 405 this advantage would carry over to triplet choice sets. Experiment 2 therefore tested whether the newly

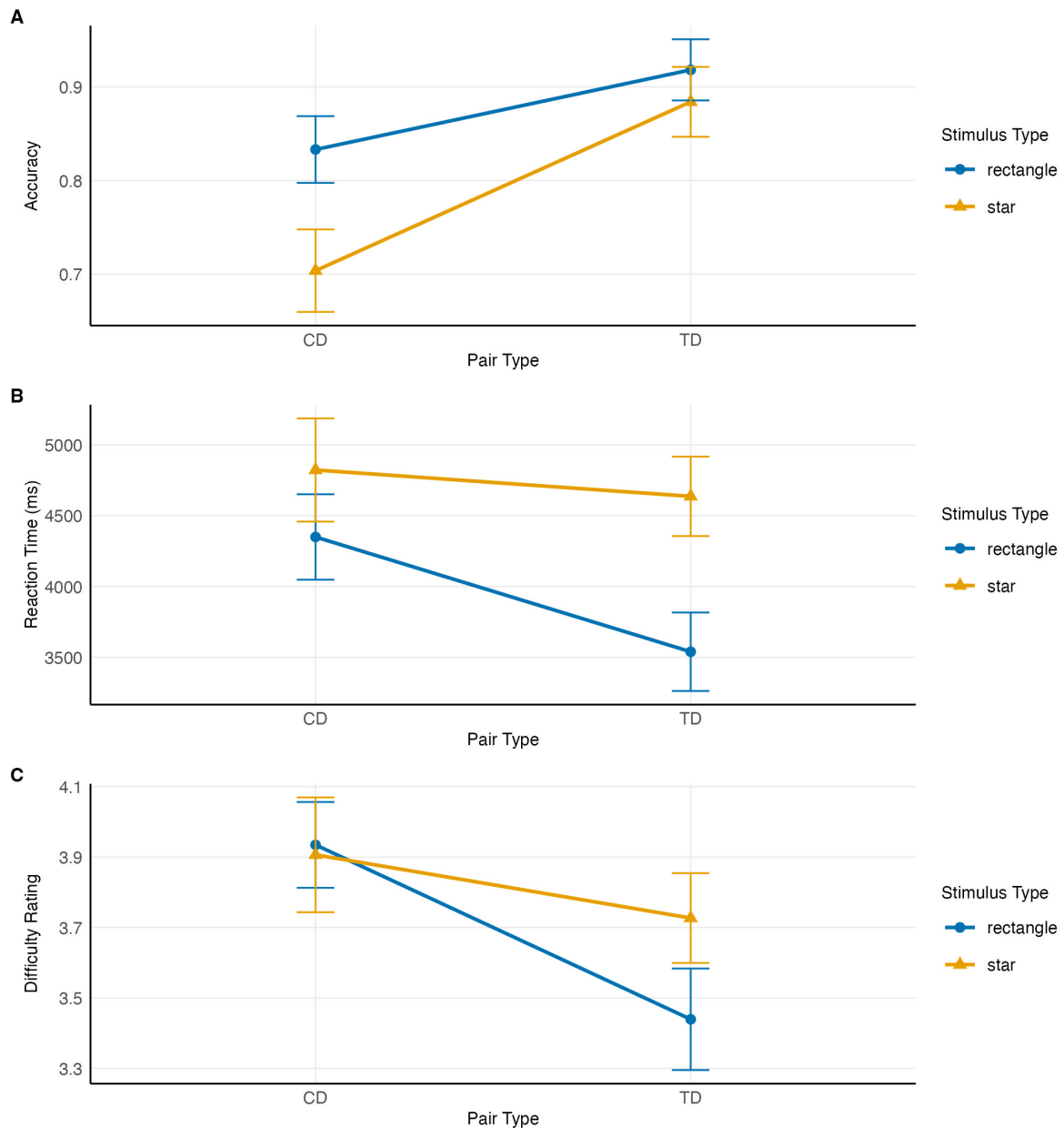


Figure 2. Interaction effects of stimulus type and pair on accuracy, reaction time, and difficulty. Error bars represent 95% within-subject confidence intervals.

406 developed star stimuli elicit a robust attraction effect in a triangular triplet arrangement, addressing prior
 407 reports of null or even reversed effects with perceptual stimuli.

3 EXPERIMENT 2

408 3.1 Introduction

409 Building on the results of Experiment 1, which showed that star stimuli produce strong asymmetric
 410 dominance in pairwise comparisons, we next asked whether this property would carry over to triplet
 411 choice sets. The assumption was that the underlying cognitive process producing asymmetric dominance
 412 in pairwise comparisons would also operate in the case of triplets and would lead to a positive attraction

413 effect. Experiment 2, therefore, tested whether the novel star-shaped stimuli generate such an effect in the
414 standard triangular configuration used in decoy paradigms.

415 3.2 Method

416 3.2.1 Participants

417 Fifty-four students (12 female) with normal or corrected-to-normal vision (M: 20.17 years, SD: 3.08,
418 range: 17-32), participated in the study.

419 3.2.2 Apparatus and Stimuli

420 The experiment was designed using JavaScript and conducted on similar laboratory computers. In each
421 trial, the stimuli consisted of three different black-colored star shapes on a white background. The three
422 stimuli (target, competitor, and decoy) were simultaneously displayed at the vertices of a virtual, upright
423 equilateral triangle centered on the display, with their vertical positions jittered across trials. The base of the
424 triangle was defined horizontally by points located at 30% and 70% of the total screen width, corresponding
425 to pixel coordinates $x = 576$ and $x = 1344$ on a 1920-pixel-wide monitor—yielding a base length of
426 768 pixels. The height of the triangle was calculated as $h = (\sqrt{3}/2) * s$, where s is the base length, resulting
427 in a height of approximately 665 pixels. The top vertex was located at the horizontal midpoint of the display
428 ($x = 960$), vertically positioned 665 pixels above the center of the base line, i.e., at $y = -125$ relative
429 to screen center ($y = 540$). The screen coordinates are defined relative to the screen center (0, 0), with
430 positive y values extending downward.

431 At a fixed viewing distance of 60 cm on a 24-inch monitor (16:9), the triangle base corresponded to
432 212.5 mm (20.1° visual angle), and its height to 184.1 mm (17.4° visual angle). Thus, the left vertex
433 was at (576, , 540), the right at (1344, , 540), and the top vertex at (960, , -125), ensuring consistent and
434 well-controlled spatial separation for all stimulus triplets across trials.

435 The star-like shapes were constructed following the method used in Experiment 1. Each star-like shape
436 had the width of the base rectangle and the height of the removed triangles as its two attributes.

437 3.2.3 Design

438 Experiment 2 employed a forced-choice design in which participants made a selection among three simul-
439 taneously presented star-like shapes, constructed to differ systematically along two attribute dimensions:
440 the width of the base rectangle and the height of the removed triangles.

441 In addition to the transition from pair to triplet comparisons, Experiment 2 incorporated a bias correction
442 that distinguished it from Experiment 1. A pilot study revealed a systematic preference among participants
443 for the wider (W) shape. To counteract this bias in the main experiment, the computed width of the narrower
444 (N) shape—denoted as w_2 —was increased by 10 pixels (See Supplementary Material Section 4). This
445 adjustment aimed to equalize the perceptual appeal of the stimuli and ensure a more balanced choice
446 distribution.

447 A total of 180 trials were administered to each participant, which took approximately 40 minutes to
448 complete. Of these, 144 were main trials, equally divided between 72 trials with the wider star shape
449 (W: wide) as the target and 72 trials with the narrower star shape (N: narrow) as the target. Additionally,
450 36 catch trials were included to assess participant-level exclusion criteria. Similar to Experiment 1, each
451 participant completed a feedback-based practice session with 10 trials before the main experiment.

452 This experimental design was chosen to maximize control over stimulus presentation, enable robust
453 counterbalancing of all conditions, and facilitate reliable statistical inference, while also accounting for
454 participant fatigue and engagement.

455 3.2.4 Procedure

456 At the start of each trial, a fixation cross appeared at the center of the screen for 500 ms. Immediately
457 thereafter, the three star-like stimuli were displayed in a triangular arrangement on a white background.
458 The stimulus display remained visible until participants made a choice response using the arrow keys; there
459 was no imposed time limit for this response. Upon selection, participants proceeded to a rating task, which

460 also remained visible until a response was made via key press, with no time restriction. After each trial, a
461 new fixation cross appeared for 500 ms before the onset of the next trial.

462 During the practice session, participants were provided feedback following each selection to help
463 familiarize them with the task. The main experiment did not include feedback. This study was not
464 preregistered.

465 3.3 Results

466 Data were collected from 54 participants. First, 11 participants were excluded due to a technical error
467 resulting in missing response time (RT) data for the majority of their trials; for these participants, only the
468 first 10 trials contained RT data, while the remaining 170 trials were missing. This technical exclusion
469 ensured data quality and left 43 participants for further analysis. Subsequently, one participant who failed
470 to meet the predefined catch trial accuracy threshold of 0.8 was excluded, resulting in a final sample of 42
471 participants.

472 Within the retained sample, all catch trials were removed from further analysis. Individual trials were
473 further excluded if their RT was less than 100 ms or exceeded 20000 ms, excluding 4.07% of main trials
474 and yielding 7,252 valid trials for subsequent analysis.

475 We quantified context effects using the equal-weights version of the Relative Choice Share of the Target
476 (RST), as defined by Katsimpokis et al. (2022), for a triplet-triplet design (Wedell, 1991). This measure
477 captures how often the target is chosen over the competitor, where an RST of 0.5 denotes no context effect.
478 Formally,

$$RST_{EW} = \frac{1}{2} \left(\frac{T_X}{T_X + C_X} + \frac{T_Y}{T_Y + C_Y} \right)$$

479 where T_X and C_X represent the target and competitor selections when the decoy favors option X, and
480 T_Y and C_Y represent these counts when the decoy favors option Y. In this context, X and Y indicate the
481 two core stimuli. Values above 0.5 indicate a bias toward the target. It should be noted that this metric that
482 is widely used for the attraction effect—change in choice probabilities with decoy introduction—is itself an
483 empirical measure of IIA violation, generally called the context effect.

484 A two-tailed one-sample t-test against 0.5 revealed that the mean RST was significantly above chance
485 ($M = 0.537$, $SD = 0.050$); $t(41) = 4.815$, $p < 0.001$, Cohen's $d = 0.723$. Complementary Bayesian
486 t-tests using the Jeffreys–Zellner–Siow prior (scale $r = 0.743$) provided strong evidence supporting the
487 alternative hypothesis ($BF_{10} = 1035.9$), indicating that the observed effect is approximately 1036 times
488 more likely under the presence of a positive context effect than under the null hypothesis.

489 To verify the robustness of these findings, we conducted extensive sensitivity analyses varying participant
490 catch trial accuracy thresholds and trial-level RT exclusion criteria. The results of these analyses are
491 reported in Supplementary Table S6, which shows that the positive context effect remains statistically
492 significant and stable across all tested exclusion permutations. Figure 3 shows two example trials and the
493 overall distribution of the choice share in the two contexts. Figure 4 depicts a corresponding violin plot for
494 the overall RST values. Further descriptive statistics on choice frequencies and response time are reported
495 in the Supplementary Material Section 7.

496 3.4 Discussion

497 To our knowledge, this study is the first to demonstrate the positive attraction effect for perceptual
498 stimuli arranged in a triangle. Experiment 2 demonstrated that the newly introduced star stimuli elicit a
499 reliable attraction effect in triplet choice sets. This finding provides direct support for the hypothesis that
500 asymmetric dominance in pairwise comparisons is a necessary precondition for the AE: the same stimuli
501 that produced strong asymmetry in dyadic judgments (Experiment 1) also yielded robust attraction in the
502 triplet format.

503 Together, Experiments 1 and 2 strengthen the case that perceptual attraction effects depend critically on the
504 presence of clear item-level dominance relations. Having established this principle with novel star stimuli,
505 we next turned to a long-standing puzzle in the literature: why rectangle stimuli, which show reliable

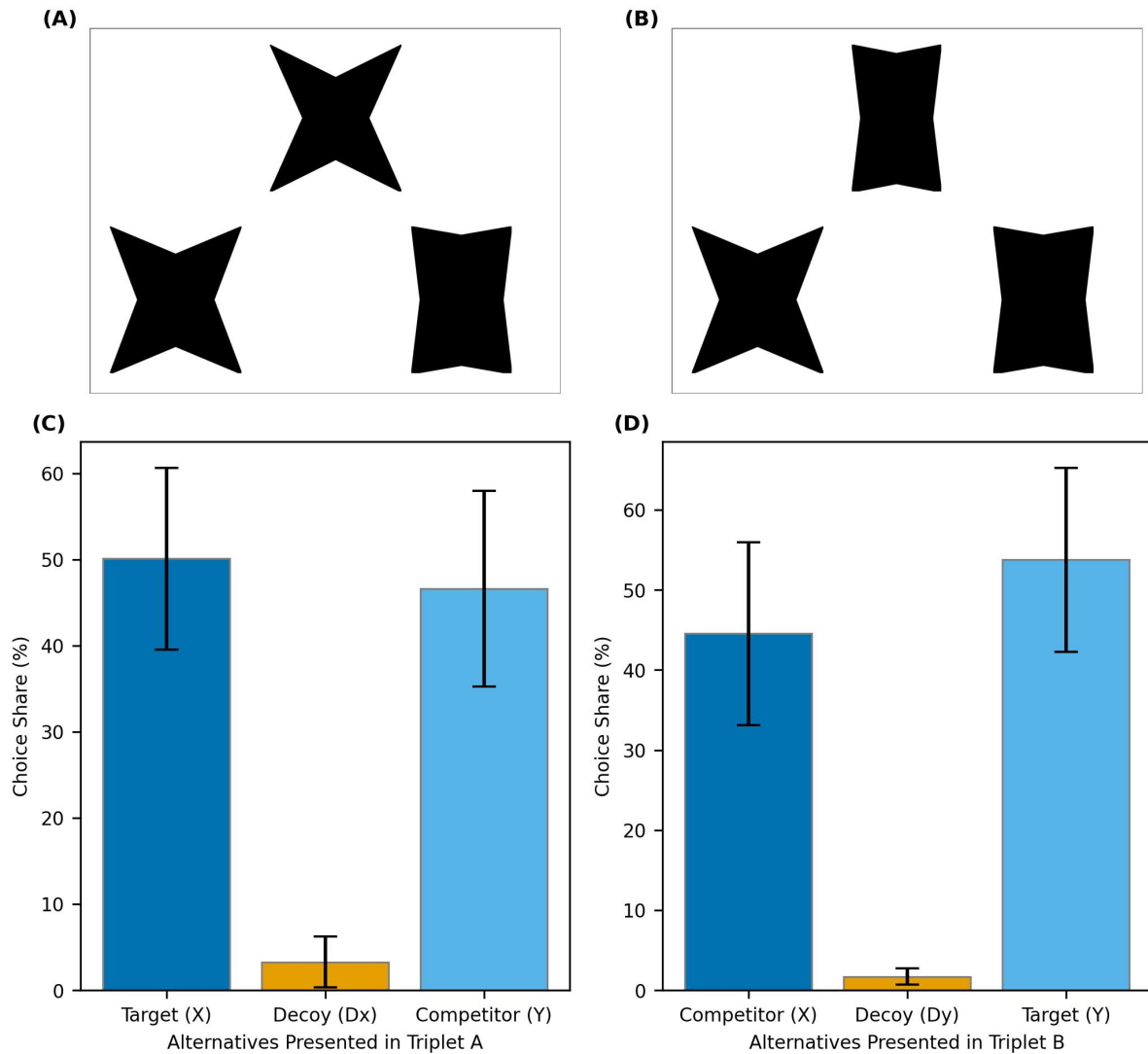


Figure 3. Example trials and choice shares in *Experiment 2*. (A) A trial where the wider stimulus serves as the target. (B) A trial where the narrower stimulus is the target. (C) Choice shares when X is the target and Dx (a decoy inferior to X) is presented. (D) Choice shares when Y is the target and Dy (a decoy inferior to Y) is presented. Error bars represent 95% within-subject confidence intervals.

506 AEs in linear arrangements, have sometimes produced reversed effects in triangular configurations. One
 507 possibility is that this puzzling outcome reflects the weaker asymmetry in decoy's dominance we observed
 508 for rectangles in pairwise tasks. Experiment 3, therefore, tested whether the apparent reversal would persist
 509 under replication, or whether it would instead resolve into a reduced—but still positive—attraction effect.

4 EXPERIMENT 3

510 4.1 Introduction

511 Experiment 3 addressed the puzzling finding that rectangle stimuli sometimes yield a reversed (negative)
 512 attraction effect in triplet choice sets (Spektor et al., 2018). Given that Experiment 1 revealed only weak
 513 asymmetric dominance for rectangles in pairwise comparisons, we predicted that in triplet set, the same
 514 stimuli should not generate a true repulsion effect but rather a reduced or null attraction effect. To test this,
 515 we ran a conceptual replication of the triangular triplet design of Spektor et al. (2018).

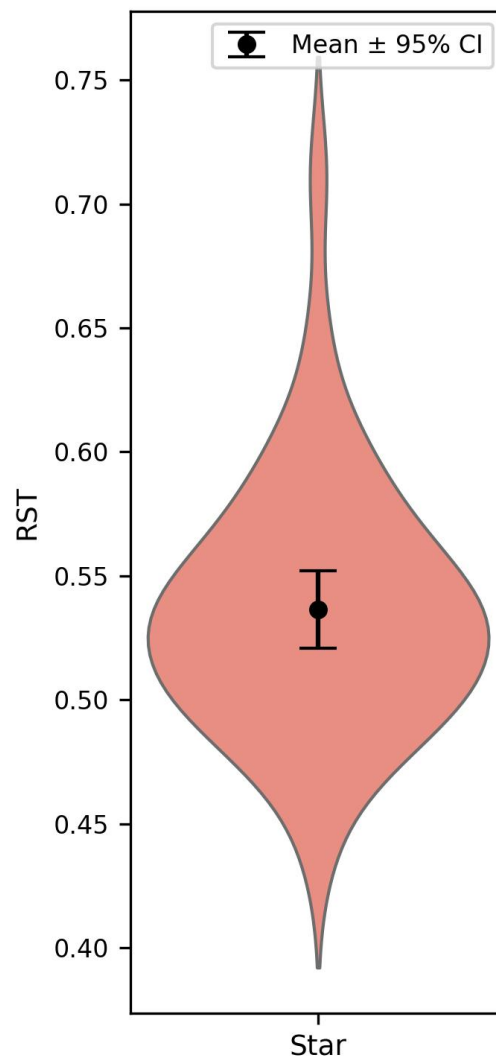


Figure 4. Relative share of the target in Experiment 3. The dot represents the mean, and the error bars indicate 95% confidence intervals based on between-subject variability.

516 In parallel, we revisited the study by [Spektor et al. \(2022\)](#), which had reported a repulsion effect with bar
517 stimuli. Their original analysis relied on RST scores collapsed across multiple within-subject manipulations,
518 raising the possibility that the observed effect reflected the interaction of these factors rather than the decoy's
519 role itself. To address this, we reanalyzed their data at the trial level, isolating the decoy manipulation.

520 The motivation for including both the direct replication and the reanalysis was two-fold. First, both
521 [Spektor et al. \(2018\)](#) and [Spektor et al. \(2022\)](#) reported negative attraction effects using perceptual stimuli.
522 We aimed to examine whether multi-attribute perceptual stimuli would produce results consistent with our
523 theoretical framework—that is, whether weak or absent asymmetric dominance would lead to null rather
524 than negative attraction effects. Second, the dataset from [Spektor et al. \(2022\)](#) is both publicly available and
525 atypical in its multi-factorial design, allowing us to test—within a model comparison framework—whether
526 the negative effect reported originally persists when all design factors are explicitly accounted for.

527 Our interpretation regarding the absence of strong asymmetric dominance of the decoys in [Spektor et al.](#)
528 [\(2022\)](#) is theoretically motivated, based on their described stimulus construction, but was not directly
529 tested within their dataset. Based on this reasoning, we anticipated that both the replication (Experiment 3)
530 and the subsequent reanalysis would yield null rather than negative effects. Under our framework, when

531 dominance asymmetry is not robustly established, we expected an absence of a context effect (i.e., a true
532 null) rather than a reversal.

533 4.2 Method

534 4.2.1 Participants

535 Seventy-six volunteers (19 female) with normal or corrected-to-normal vision (M : 20.93 years, SD : 2.56,
536 range: 17–28), participated in the experiment.

537 4.2.2 Apparatus and Stimuli

538 This experiment was designed using JavaScript and conducted on the same laboratory computers as in
539 previous experiments. Rectangle stimuli were created following the procedures described in Experiment
540 1, and the decoy construction method (including range, frequency, and range-frequency decoys) was
541 consistent with Experiment 1. The spatial arrangement and display calibration for stimulus presentation
542 were identical to Experiment 2; that is, on each trial, three stimuli were simultaneously displayed at the
543 vertices of an upright, virtual equilateral triangle centered on the screen (see Section 3.2.2, Apparatus and
544 Stimuli, Experiment 2, for full geometric and display details).

545 4.2.3 Design

546 Experiment 3 employed a forced-choice design in which participants made a selection among three
547 simultaneously presented rectangles, each differing in area. The arrangement of rectangles and decoy
548 generation methods (range, frequency, and range-frequency decoys) were matched to those used in
549 Experiment 1 to enable direct comparison across experiments.

550 A total of 162 trials were presented to each participant. These trials included 144 main trials and 18 catch
551 trials, ensuring all conditions were fully counterbalanced.

552 The trial count was determined to balance robust data quality with participant comfort and engagement.
553 Randomization of trial presentation ensured that each participant experienced every condition, supporting
554 reliable statistical inference.

555 4.2.4 Procedure

556 At the start of each trial, a fixation cross appeared at the center of the screen for 500 ms. Immediately
557 thereafter, three rectangle stimuli were displayed in a triangular formation on a white background. Par-
558 ticipants were instructed to select the rectangle with the largest area. The stimulus display remained on
559 the screen until the participant made a choice response by pressing the corresponding key; there was no
560 imposed time limit for this response. After selection, the next trial began following a 500 ms fixation
561 interval.

562 Practice trials were presented at the beginning of the session, during which participants received feedback
563 after each response to familiarize them with the task requirements. No feedback was provided during the
564 main experiment. This study was not preregistered.

565 4.3 Results

566 Of the 76 participants tested, two were excluded due to a technical error that prevented complete reaction
567 time (RT) logging. An additional six participants were excluded for performing below the predetermined
568 accuracy threshold (i.e., less than 80%) on catch trials.

569 At the trial level, responses with implausible RTs were excluded. Specifically, trials with RTs below
570 100 ms or exceeding 20000 ms were removed. This procedure led to the exclusion of 126 trials, representing
571 approximately 1.14% of the total data, and resulted in 10892 valid trials available for analysis.

572 We performed a two-tailed one-sample t -test on the overall RST. We were unable to replicate the negative
573 AE reported in previous studies; rather, we found that overall RST ($M = 0.500$, $SD = 0.053$) was not
574 significantly different from the null (0.5); $t(67) = 0.029$, $p = 0.98$, Cohen's $d = 0.004$. To further quantify
575 the evidence, we conducted a Bayesian one-sample t -test using the default Jeffreys–Zellner–Siow (JZS)
576 prior with a scale parameter $r = 0.707$. The Bayes factor ($BF_{10} = 0.13$) indicated that the data were about
577 seven times more consistent with the null hypothesis than with the alternative. Figure 5 shows the overall

578 distribution of the choice share in the two contexts, and Figure 6 depicts a corresponding violin plot for
 579 the overall RST values. Robustness checks paralleling those conducted in Experiment 2—varying both
 580 participant-level and trial-level exclusion thresholds—consistently supported the null hypothesis across all
 581 tested parameters (Supplementary Table S7), confirming that the lack of a context effect in Experiment 3
 582 reflects a genuine absence rather than an artifact of data filtering. Further descriptive statistics on choice
 583 frequencies and response times are also reported in the Supplementary Material Section 7.

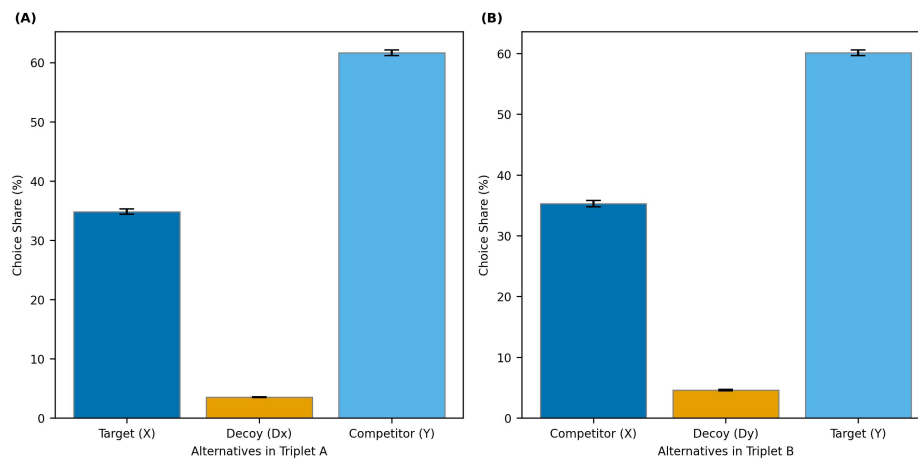


Figure 5. Choice shares in *Experiment 3* for the two triplet contexts. (A) Choice shares when X is the target and Dx (a decoy inferior to X) is presented in Triplet A. (B) Choice shares when Y is the target and Dy (a decoy inferior to Y) is presented in Triplet B. Error bars represent 95% within-subject confidence intervals calculated using the Cousineau-Morey method.

584 4.3.1 Re-analysis of [Spektor et al. \(2022\)](#)

585 Because bar stimuli have previously yielded reversed attraction effects, we conducted a re-analysis of
 586 the original data from [Spektor et al. \(2022\)](#). That study manipulated several design factors simultaneously,
 587 making it difficult to isolate the role of any single manipulation. We therefore compared a set of competing
 588 models, including a null model, a baseline additive model, and multiple interaction models. The best-fitting
 589 Generalized Linear Mixed-Effects Model (GLMM) yielded a non-significant estimate for the target variable
 590 (see Supplementary Material Section 4 for details). This pattern is most consistent with a null attraction
 591 effect.

592 Experiment 3 tested whether rectangles, which had previously been reported to elicit a negative attraction
 593 effect in triangular arrangements ([Spektor et al., 2018](#)), would reproduce this pattern. Instead, we observed
 594 a null effect: neither a reliable positive nor a negative attraction effect emerged. This finding suggests that
 595 the relationship between stimulus geometry and the attraction effect is not straightforward. Rectangles
 596 produced weak but significant dominance asymmetries in pairwise comparisons (Experiment 1) and have
 597 reliably supported the attraction effect in linear arrangements in prior work ([Trueblood et al., 2013](#)), yet in
 598 triangular displays they failed to produce the effect.

599 The re-analysis of [Spektor et al. \(2022\)](#) provided converging evidence. Although their original report
 600 suggested a repulsion effect, this was based on analyses collapsing across multiple within-subject manip-
 601 ulations. By isolating the decoy's contribution with a trial-level GLMM approach, we found no reliable
 602 attraction or repulsion effect. While we did not directly test whether the bar stimuli used in their study
 603 achieved item-wise dominance asymmetry, our interpretation of these results is theoretically grounded
 604 in the assumption—based on their stimulus construction—that such dominance asymmetry was likely
 605 weak or absent. Together, the replication and the re-analysis support the conclusion that when dominance
 606 asymmetry is not robustly established, the expected outcome is a true null effect, rather than a reversal of
 607 the attraction effect.

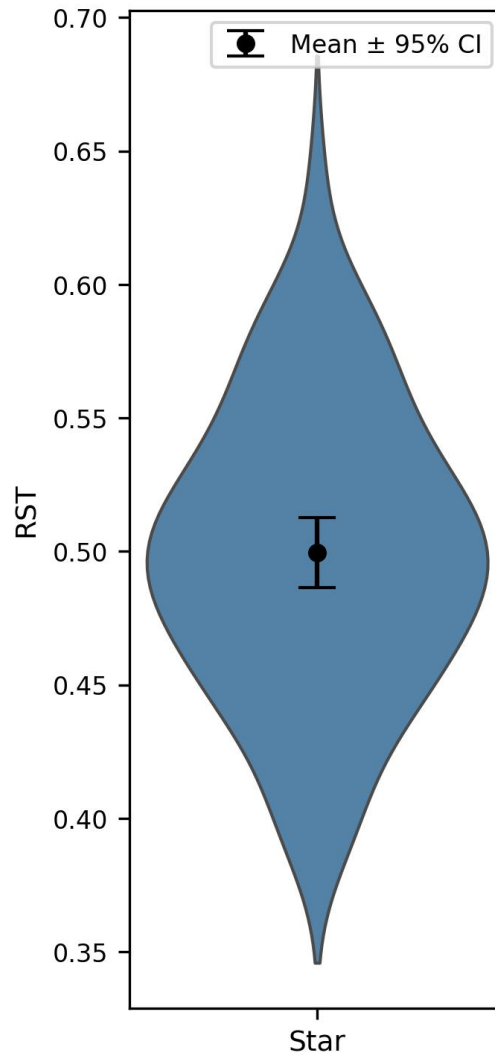


Figure 6. Relative share of the target in *Experiment 3*. The dot represents the mean, and the error bars indicate 95% confidence intervals based on between-subject variability.

608 4.4 Discussion

609 Taken together, the replication and reanalysis reinforce the conclusion that AE depends not only on the
610 presence of asymmetric dominance but also on how spatial arrangements channel attention to target–decoy
611 versus competitor–decoy relations. A linear layout may enhance the accessibility of these comparisons,
612 whereas triangular arrangements may dilute or redistribute attentional salience across pairs.

613 Overall, Experiments 1–3 suggest that AE is not guaranteed by perceptual decoys alone: it requires the
614 structural condition of item-based dominance asymmetry. This raises a critical next question: does spatial
615 alignment of options interact with the underlying cognitive processes to produce dominance asymmetry?
616 Experiment 4 was designed to test this possibility.

5 EXPERIMENT 4

617 5.1 Introduction

618 Across Experiments 1–2, our findings converged on the idea that the attraction effect (AE) critically
619 depends on the decoy's dominance asymmetry. When decoys created strong asymmetry in pairwise
620 comparisons, as with our novel star stimuli, we observed both clear pairwise asymmetries (Exp. 1) and

robust AE in triplet choices (Exp.2). Moreover, in Experiment 3, the null attraction effects—both in our reanalysis of bar stimuli and in the failed replication of rectangles in triangular displays (Spektor et al., 2018, 2022)—shift the interpretation away from accounts based on a repulsion effect and instead toward a boundary condition defined by the presence or absence of asymmetric dominance. Rectangles presented a more intriguing case: they produced significant asymmetry in pairwise comparisons (Exp. 1) and reliably elicited AE in linear triplet arrangements in prior work, yet failed to do so in triangular arrangements (Exp. 3). This discrepancy raises a key question: why should display layout matter at all?

It is important to note that Experiment 1 involved rectangle pairs presented in linear horizontal alignment. It is also noteworthy that in a triangular arrangement with equal representation of all six possible (T, C, D) configurations, each participant encounters one-third of trials where both TD and CD pairs are oblique, one-third where the TD pair is horizontal and the CD pair is oblique, and one-third where the CD pair is horizontal and the TD pair is oblique. This ensures that in triangular display, the attentional advantages are distributed across conditions, potentially diluting the overall dominance asymmetry. By contrast, linear triplets always contain horizontally aligned pairs, potentially amplifying dominance asymmetry in favor of the target.

One possibility, then, is that linear arrangements introduce systematic attentional biases. For instance, the central item always appears at fixation, and transitions between horizontally adjacent items may be easier than between outer items (Spektor et al., 2022). Moreover, matched orientations in a linear alignment may make target–decoy (TD) pairs consistently salient, regardless of their specific positions. This assumption is reasonable. Indeed, the Multi-attribute Linear Ballistic Accumulator (MLBA) model (Trueblood et al., 2014; Turner et al., 2018; Evans et al., 2019) makes a similar assumption to explain the same positive effect in the linear alignment of rectangle stimuli. According to the model, the relative salience of pairwise comparisons drives the AE: TD comparisons are weighted more strongly than competitor–decoy (CD) comparisons because of attribute similarity, which favors the target. More general frameworks (Trueblood et al., 2022) extend this idea by allowing attentional weights to be modulated by factors such as attribute bias or presentation format. Although these models can retrospectively attribute differences in AE to spatial modulation of attentional weights, existing explanations remain inferential, hinging on untested assumptions about attention allocation.

Psychophysical research strengthens this prediction. Across diverse paradigms, horizontally aligned stimuli enjoy processing advantages—faster reaction times, lower perceived difficulty, and stronger attentional capture—relative to oblique or vertical alignments (Chen et al., 2019; Tsal, 1989). Yet, choice-based studies of context effects have not directly tied these perceptual benefits to the underlying attentional weights that determine preference construction. Thus, a direct behavioral test of whether spatial alignment affects the ease of TD versus CD comparisons remains missing.

Experiment 4 addresses this gap by directly measuring the perceived difficulty of TD and CD comparisons under two alignment conditions: horizontal (linear) and oblique. By asking participants to rate difficulty in addition to making choices, we isolate attentional salience mechanisms and empirically test the key assumption that spatial alignment modulates attentional weights.

Unlike Experiment 1, where the main hypotheses concerned choice behavior—since dominance asymmetry was naturally defined in terms of accuracy—the present experiment focused on subjective difficulty ratings. In Experiment 4, we operationalized the attentional salience of each stimulus pair through the perceived difficulty of pairwise comparisons. This approach enabled us to quantify salience differences between Target-Decoy (TD) and Competitor-Decoy (CD) pairs in different alignments.

Hypotheses:

1. **Main effect of Pair Type:** TD comparisons will be rated as easier than CD comparisons.
2. **Main effect of Alignment:** Horizontal comparisons will be rated as easier than oblique comparisons, reflecting the horizontal attention advantage.
3. **Interaction:** The TD–CD ease advantage will be greatest when comparisons are horizontally aligned. This advantage should be attenuated when comparisons are presented obliquely; if spatial alignment systematically favors CD over TD, the TD–CD difference may be further reduced.

671 5.2 Method

672 5.2.1 Participants

673 Forty-two university students (9 female) with normal or corrected-to-normal vision (M: 21.45 years, SD:
674 2.86, range: 17-27), participated in the experiment.

675 5.2.2 Apparatus and Stimuli

676 Experiment 4 was conducted on a 24-inch, 1920 × 1080-pixel monitor (16:9) viewed at approximately
677 60 cm, with all display calibration, rectangle-based stimulus generation, and attribute matching procedures
678 identical to those described in Experiment 1. Stimuli were presented as black rectangles on a white
679 background.

680 The spatial configuration of each stimulus pair followed the virtual equilateral triangle arrangement
681 detailed for Experiments 2 and 3 (see Apparatus and Stimuli, Experiments 2–3). On each trial, two
682 rectangles were simultaneously displayed at two of the three vertices of the triangle (left-top, right-top, or
683 left-right combinations). The vertex coordinates, triangle base and height, and corresponding visual angles
684 were as previously specified: base at $x = 576$ and $x = 1344$ (768 pixels/212.5 mm/20.1°), top at ($x = 960$,
685 $y = -125$), triangle height 665 pixels (184.1 mm/17.4°). This ensured that spatial separation, size, and
686 visual angle were strictly comparable to those in earlier experiments.

687 5.2.3 Design

688 Experiment 4 employed a within-subjects forced-choice design in which participants selected the rectangle
689 with the larger area from two simultaneously presented stimuli. Each trial consisted of either a Target–Decoy
690 (TD) or a Competitor–Decoy (CD) pair, constructed from the corresponding triplets used in previous
691 experiments.

692 For every combination of *Pair Type* (TD or CD) and *trial type* (range, frequency, range–frequency), four
693 spatial presentation variants were used: *aligned0*, *aligned1*, *oblique0*, and *oblique1*. On each trial, only two
694 of the three triangle vertices were occupied by rectangles. For CD pairs, aligned variants corresponded to
695 the Competitor (C) and Decoy (D) occupying the left and right base vertices (aligned0: C left, D right;
696 aligned1: D left, C right). Oblique variants corresponded to one item at a base vertex and the other at the
697 top vertex (oblique0: C left, D top; oblique1: C right, D top). The same assignment logic was employed for
698 TD pairs. For the final analysis, both aligned variants were combined into a single category, “aligned,” and
699 both oblique variants were combined into “oblique.”

700 This design yielded 24 total experimental trials per participant, with presentation order fully randomized.
701 Each trial also included a difficulty rating task following the choice response. The number of trials was
702 chosen to balance comprehensive coverage of all spatial arrangements with participant comfort, given the
703 inclusion of rating tasks and the precision required for spatial positioning judgments.

704 5.2.4 Procedure

705 At the start of each trial, a fixation cross appeared at the center of the screen for 500 ms. Immediately
706 thereafter, two rectangle stimuli were displayed at the designated triangle vertices on a white background.
707 The stimulus display remained visible until the participant made a choice response via key press; there was
708 no imposed time limit for this response. Upon making their selection, participants proceeded to a rating
709 task in which they rated the difficulty of their decision on a 7-point Likert scale, where one represented
710 “extremely easy” and seven represented “extremely difficult.” The rating display also remained visible
711 until a response was recorded via key press, with no time restriction. After each trial, a new fixation cross
712 appeared for 500 ms before the onset of the next trial.

713 5.3 Results

714 Data from all forty-two participants were analyzed. We first applied the same duration exclusion criteria
715 as preregistered in Experiment 1 (removing trials shorter than 100 ms or longer than 20 s), which resulted
716 in the exclusion of 2.37% of trials.

717 A two-way repeated-measures ANOVA with *Pair Type* (TD vs. CD) and *Presentation Alignment* (aligned
718 vs. oblique) as within-subject factors was conducted on participants’ difficulty ratings. The analysis revealed

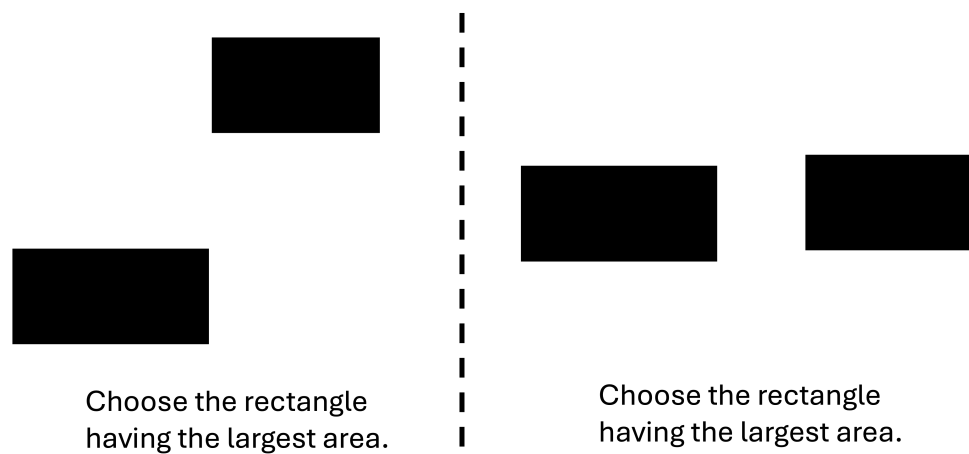


Figure 7. Example Trials in Experiment 4. Stimuli pair are in oblique and horizontally aligned positions from left to right

719 a main effect of Pair Type, with TD comparisons rated as easier than CD comparisons, $F(1, 41) = 27.22$,
 720 $p < .001$, $\eta_p^2 = .40$. There was also a main effect of Presentation Alignment, with horizontal (aligned)
 721 comparisons rated as easier than oblique comparisons, $F(1, 41) = 29.19$, $p < .001$, $\eta_p^2 = .42$. Importantly,
 722 these effects were qualified by a significant interaction between Pair Type and Presentation Alignment,
 723 $F(1, 41) = 5.21$, $p = .028$, $\eta_p^2 = .11$ (see Figure 8). To verify that the observed interaction was not
 724 driven by specific exclusion criteria, we conducted a sensitivity analysis similar to those employed in
 725 previous experiments, varying participant accuracy thresholds and trial-level RT cutoffs. As summarized
 726 in Supplementary Table S8, all main and interaction effects for our primary variable, difficulty rating,
 727 remained significant and stable across all tested parameter combinations.

728 Descriptive statistics are summarized in Table 3. CD comparisons were rated as more difficult (aligned:
 729 $M = 4.09$, $SD = 1.05$; oblique: $M = 4.35$, $SD = 0.91$) than TD comparisons (aligned: $M = 3.38$,
 730 $SD = 0.96$; oblique: $M = 3.94$, $SD = 0.97$).

731 To probe the interaction, we conducted four planned pairwise comparisons with Holm–Bonferroni
 732 correction (Table 4). TD–CD differences were significant in both the aligned ($t(41) = -4.99$, $p_{\text{holm}} < .001$,
 733 $d_z = -0.77$) and oblique conditions ($t(41) = -3.87$, $p_{\text{holm}} < .001$, $d_z = -0.60$). The strongest difference
 734 was between TD-aligned and CD-oblique ($t(41) = -6.95$, $p_{\text{holm}} < .001$, $d_z = -1.07$). By contrast,
 735 CD-aligned and TD-oblique did not differ reliably ($t(41) = 1.24$, $p_{\text{holm}} = .222$, $d_z = 0.19$). This pattern is
 736 consistent with our hypotheses: the TD–CD asymmetry advantage was maximal under horizontal alignment
 737 and attenuated under oblique alignment.

738 Additionally, when accuracies were collapsed across presentation formats, no meaningful difference
 739 was observed between TD ($M = 0.870$, $SD = 0.167$) and CD ($M = 0.850$, $SD = 0.145$) conditions. A
 740 Wilcoxon signed-rank test indicated no significant difference in accuracy between TD and CD trials
 741 ($W = 286$, $p = .277$). A paired-samples t -test showed a consistent pattern, $t(41) = 1.16$, $p = .254$,
 742 Cohen's $d = 0.18$. Further descriptive and inferential statistics for accuracy and reaction times are reported
 743 in the Supplementary Material (Section S7, Table S12–S14) for completeness.

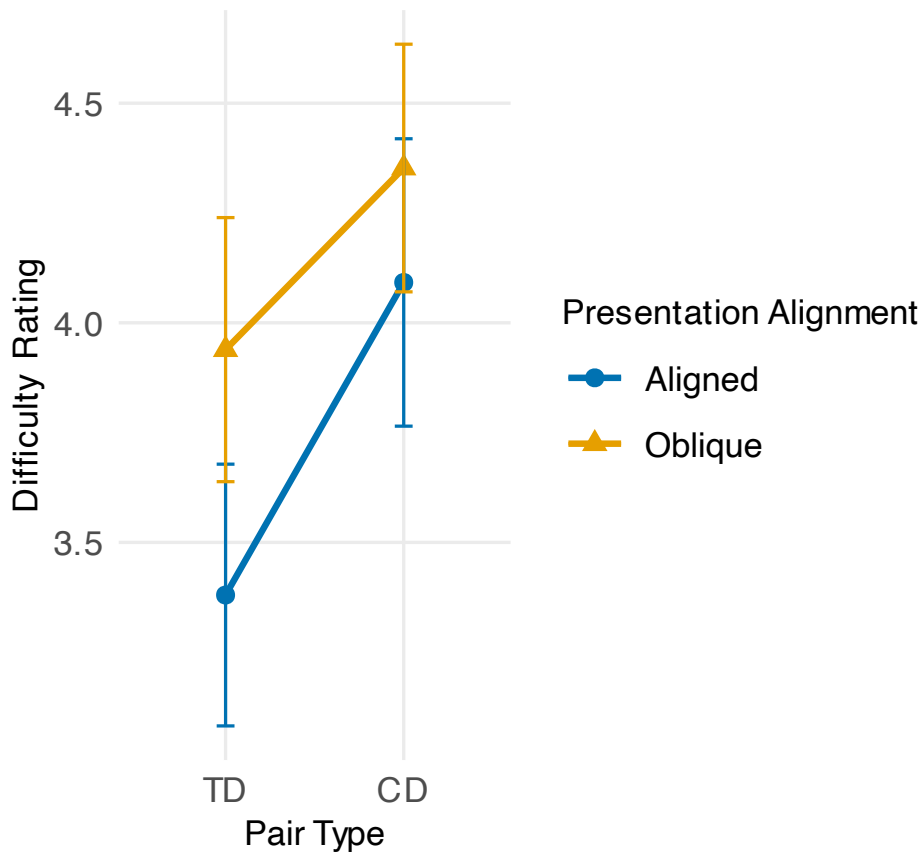


Figure 8. Mean difficulty ratings in Experiment 4 as a function of Pair Type (TD vs. CD) and Presentation Alignment (horizontal vs. oblique). Error bars indicate 95% confidence intervals of the mean (within-subject). The interaction reflects that the TD–CD ease advantage was more pronounced in the horizontal condition and attenuated in the oblique condition.

Table 3. Mean difficulty ratings (M) and standard deviations (SD) by condition.

Condition	M	SD
CD aligned	4.09	1.05
CD oblique	4.35	0.91
TD aligned	3.38	0.96
TD oblique	3.94	0.97

Table 4. Planned pairwise comparisons of difficulty ratings in Experiment 4. p -values are Holm–Bonferroni corrected.

Contrast	$t(41)$	p_{holm}	d_z	95% CI
TD aligned vs. CD aligned	-4.99	< .001	-0.77	[-1.11, -0.42]
TD oblique vs. CD oblique	-3.87	< .001	-0.60	[-0.92, -0.26]
TD aligned vs. CD oblique	-6.95	< .001	-1.07	[-1.45, -0.69]
CD aligned vs. TD oblique	1.24	.222	0.19	[-0.11, 0.50]

744 Discussion

745 Unlike Experiment 1, in Experiment 4 the rectangles clearly lacked an item-wise asymmetric dominance
 746 of decoys in terms of choice accuracies. Beyond accuracy, Experiment 4 evaluated attentional biases as
 747 indexed by subjective difficulty ratings, which capture participants' relative ease of processing pairs under
 748 different spatial arrangements. It provided direct evidence that the accessibility of asymmetric dominance

749 depends on spatial alignment. As predicted, TD comparisons were rated as easier than CD comparisons.
750 We also observed a main effect of alignment, with horizontally aligned comparisons rated as easier than
751 oblique ones, consistent with prior psychophysical work on horizontal processing advantages. Crucially,
752 these two effects interacted: the TD–CD ease difference was strongest for horizontal pairs and attenuated
753 for oblique pairs.

754 These findings help reconcile the puzzling discrepancy observed with rectangles. Rectangles, in Ex-
755 periment 1, produced detectable pairwise asymmetry and produced robust AE in linear arrangements in
756 prior studies, but they failed to yield AE in triangular displays (Experiment 3). Experiment 4 suggests a
757 principled explanation: the weaker dominance asymmetry inherent to rectangles becomes accessible and
758 behaviorally consequential only when supported by horizontal alignment. In triangular layouts, where
759 TD and CD pairs are frequently oblique, this asymmetry is perceptually harder to access, undermining
760 the conditions for AE to emerge. More broadly, our findings indicate that asymmetric dominance, as a
761 condition, is also dependent on attentional weighing of pairwise comparisons.

6 GENERAL DISCUSSION

762 The present research set out to clarify the conditions under which the attraction effect (AE) emerges and to
763 identify the mechanisms that drive it. By combining four experiments with reanalyses of prior work, we
764 examined how item-based dominance asymmetries and presentation factors shape both pairwise judgments
765 and multi-option choices. Our findings highlight the central role of asymmetric dominance as a boundary
766 condition in producing AE, while also pointing to possible cognitive processes that manifest this boundary
767 condition. In what follows, we summarize the main results, outline their theoretical implications, note
768 methodological contributions, and discuss limitations and future directions.

6.1 Summary of Findings

770 Across four experiments, we systematically investigated when and why the attraction effect (AE) emerges.
771 A consistent pattern was observed: AE is closely tied to asymmetric dominance in pairwise comparisons.
772 When stimuli such as stars produced strong dominance asymmetry of decoys, we observed both reliable
773 asymmetries in pairwise judgments (Experiment 1) and robust AE in triplet choices (Experiment 2). By
774 contrast, a reanalysis of prior work with bar stimuli (Spektor et al., 2022) showed no AE in triplets.
775 Rectangles presented a more nuanced case: they produced clear asymmetry in pairwise comparisons
776 (Experiment 1) and elicited AE in linear triplets in past studies, but failed to show AE in triangular
777 arrangements (Experiment 3). Experiment 4 further clarified this discrepancy. Item-wise asymmetric
778 dominance of decoys disappeared when rectangle pairs were presented in both horizontally aligned and
779 oblique arrangements. At the same time, Experiment 4 showed that participants perceived target–decoy (TD)
780 comparisons as easier than competitor–decoy (CD) comparisons overall, and that horizontal arrangements
781 selectively enhance this perceived ease advantage. Together, these findings offered a coherent explanation
782 for the mixed results involving rectangles.

6.2 Theoretical Implications

784 Our findings have several important theoretical implications for understanding the attraction effect and
785 decision-making processes more broadly. First, they provide strong support for the item-based definition
786 of asymmetric dominance originally proposed by Huber et al. (1982) as a prerequisite for the attraction
787 effect. While much of the subsequent literature has adopted an attribute-based definition focused on specific
788 attribute comparisons, our results suggest that the original, more general item-based conceptualization
789 better captures the conditions necessary for producing the attraction effect. This account explains why stars
790 consistently yield robust AE, while other stimuli, when they lack systematic dominance asymmetry, fail
791 to produce it. In this sense, AE is best understood as a consequence of structural asymmetries, not as a
792 universal artifact of decoy presence.

793 Second, our results help resolve apparent contradictions in the literature regarding the domain generality
794 of the attraction effect. The failure to observe positive attraction effects in perceptual tasks with triangular
795 arrangements (Spektor et al., 2018, 2021, 2022) had called into question whether the effect generalizes
796 beyond higher-level decision domains. By demonstrating robust AE with perceptually complex stimuli

797 (e.g., stars), our findings suggest that the attraction effect is indeed domain-general, but critically dependent
798 on the presence of item-level dominance asymmetries.

799 Third, our item-based asymmetric dominance framework offers new insight into other established bound-
800 ary conditions for the attraction effect. Previous work has demonstrated that attraction effects are attenuated
801 or even abolished when attributes are commensurable—that is, when they can be directly compared on a
802 common scale (Hayes et al., 2024; Banerjee et al., 2024b). Within our framework, commensurability likely
803 facilitates holistic or integrated evaluation, wherein attributes are combined into a common currency or
804 composite value before comparison. This process reduces the effective item-level dominance asymmetry of
805 the decoy, as the decoy's attribute-wise advantage over the competitor may be offset by other attributes
806 during integration. As a result, the key dominance-asymmetry boundary condition for robust attraction is
807 weakened. Thus, our account suggests that the effects of commensurability arise primarily by suppressing
808 dominance asymmetry, rather than via a separate cognitive process, unifying these phenomena within a
809 single explanatory framework.

810 Furthermore, our dominance asymmetry framework offers a compelling explanation for the zero attraction
811 effect observed by Trendl et al. (2021) using naturalistic movie stimuli. Their study represents a particularly
812 instructive case because it rigorously satisfied all boundary conditions identified by Huber et al. (2014),
813 yet still failed to demonstrate any attraction effect. Trendl et al. (2021) concluded that “the attraction
814 effect is limited to choice tasks where options are represented in a stylized format with objectively
815 defined attributes,” but our findings suggest an alternative explanation grounded in the absence of genuine
816 dominance asymmetry.

817 Crucially, while Trendl et al. (2021) carefully constructed their stimuli to ensure that decoys were clearly
818 dominated—with decoys rated at least three points lower than both targets and competitors on seven-point
819 scales—they failed to establish the asymmetric dominance relationships that our work identifies as essential.
820 Their experimental design explicitly created target–decoy pairs with “many shared genres that are likely to
821 be perceived as similar” while ensuring “target–competitor pairs with no genre overlap that are likely to
822 be perceived as different.” This design choice, while methodologically sound for establishing dominance,
823 inadvertently created conditions for symmetric rather than asymmetric dominance.

824 Under our framework, the zero attraction effect in Trendl et al. (2021)'s study reflects not the inherent
825 limitations of naturalistic stimuli, but rather the absence of the critical boundary condition we identify:
826 genuine item-level dominance asymmetry. Their decoys were symmetrically dominated by both targets
827 and competitors, violating the fundamental requirement that decoys must create stronger dominance
828 relationships with targets than with competitors. The fact that participants correctly identified and avoided
829 decoys (choosing them in only 4.3% of trials) confirms that dominance was perceived; however, the
830 symmetric nature of this dominance eliminated the differential comparison advantage that drives attraction
831 effects.

832 This interpretation suggests that naturalistic stimuli can theoretically support attraction effects when
833 dominance asymmetry conditions are met. The challenge lies in constructing naturalistic choice sets
834 where decoys are more clearly dominated by targets than by competitors—a task that may require careful
835 attention to attribute structure and similarity relationships that go beyond traditional experimental design
836 considerations. Trendl et al. (2021)'s findings thus provide strong convergent evidence for our theoretical
837 framework: attraction effects emerge when decoys create asymmetric rather than merely symmetric
838 dominance relationships, regardless of stimulus type or domain.

839 The case of rectangles further refined our theoretical understanding. While the presence or absence of
840 dominance asymmetry in pairwise comparisons could explain the presence or absence of AE in rectangle
841 triplets, at the process level, we found an interaction between the differential ease of comparison in specific
842 item pairs (TD vs CD) and the presentation format. A speculative explanation is axis-congruence: because
843 rectangles have width and height as defining attributes and are naturally encoded along orthogonal axes
844 (in our case, horizontal and vertical axes), their evaluation may depend on whether these axes align with
845 the spatial arrangement of options. When alignment is congruent (e.g., linear layouts), TD comparisons
846 are facilitated, whereas incongruence (e.g., oblique triangular layouts) may reduce accessibility. This
847 explanation is speculative and likely specific to rectangles or even bars, due to their attribute structures.
848 Importantly, it remains an open question whether other visual perceptual stimuli would show similar
849 susceptibility.

850 While we did not observe aggregate-level repulsion (reversed attraction) effects in any of our experiments,
851 the existence of repulsion effects is robustly documented in the literature, either in the traditional regularity
852 violation terms (Spektor et al., 2018, 2022; Banerjee et al., 2024a) or in broader operationalization—where
853 instead of 3 alternative forced choice, a rank order of preference is recorded with decoys that are objectively
854 superior and frequently chosen (Dumbalska et al., 2020). By carefully designed attribute structure and
855 stimulus design, it may be possible to induce the negative attraction effect (still violating the regularity
856 principle). Importantly, our theoretical framework extends to these phenomena: by incorporating attentional
857 weights into the ordinal pairwise comparison model, the framework can account for how presentation
858 format and context-dependent attention can shift the balance of subjective comparisons, thus explaining
859 both standard attraction and its reversal—the repulsion effect—in certain choice contexts.

860 6.3 Methodological Contributions

861 This study makes several methodological contributions to the field of decision-making research. We
862 introduced a novel perceptual stimulus—the star-shaped figure—that effectively creates conditions for
863 asymmetric dominance. This stimulus design offers researchers a new tool for investigating the attraction
864 effect in perceptual domains while maintaining the critical feature of dominance asymmetry. The effective-
865 ness of this stimulus derives from its complex perceptual properties that require integrating multiple visual
866 features, thereby creating conditions where dominance relationships between alternatives become more
867 pronounced.

868 Our methodological approach also demonstrates the importance of verifying dominance asymmetry at
869 the pairwise level before implementing decoy paradigms. The underlying assumption that the process
870 responsible for dominance asymmetry structure in pairwise comparisons would also operate in the triplet
871 set to favor the target was supported by our findings. The design in Experiment 1, directly comparing
872 accuracy in TD versus CD pairs, provided a template for researchers to validate stimulus sets prior to testing
873 AE in full triplet contexts. This validation step may be particularly valuable when working with perceptual
874 stimuli where dominance relationships may be less intuitive than in value-based decision-making.

875 Additionally, by directly comparing different stimulus types (stars, bars, rectangles) within the same
876 experimental paradigm, our experiments provide a controlled demonstration of how stimulus properties
877 may influence dominance asymmetry and, in turn, the emergence of AE. This comparative approach could
878 be extended to other types of stimuli to further map the boundary conditions of the effect.

879 Methodologically, our work also advances the literature by combining multiple behavioral measures:
880 pairwise comparisons, triplet choices, and subjective difficulty ratings (Experiment 4). This triangulation
881 allowed us to connect perceptual asymmetries observed in simple comparisons to the aggregate choice
882 patterns observed in more complex sets, thereby providing converging evidence that AE is grounded in the
883 psychological experience of comparative ease rather than being a statistical artifact of choice proportions.

884 Finally, we integrated new experimental evidence with reanalyses of existing datasets (e.g., Spektor
885 et al. (2018)). This combination of replication, extension, and synthesis increases confidence in the
886 robustness of our conclusions while also clarifying why prior findings sometimes appeared inconsistent.
887 Specifically, our results show that apparent contradictions are better understood as reflecting stimulus- and
888 arrangement-specific boundary conditions, rather than a fundamental instability of AE itself.

889 6.4 Limitations and Future Directions

890 Despite its contributions, this work has several limitations that suggest important avenues for future
891 research. First, while our novel star stimuli successfully produced dominance asymmetry and a reliable
892 attraction effect, the specific properties that make these stimuli effective remain underspecified. A stronger
893 dominance asymmetry could itself be a result of attribute incommensurability (Walasek and Brown, 2023;
894 Hayes et al., 2024). Future research could systematically vary stimulus properties to identify which features
895 are critical for generating effective asymmetric dominance in perceptual tasks.

896 Second, our findings with rectangles illustrate that attraction effects are not uniformly robust across
897 stimulus types or presentation formats. The weaker but significant asymmetry of dominated decoys in
898 horizontally presented pairwise comparisons vanished when pairs were distributed in horizontally aligned
899 and oblique arrangements—a result that directly highlights the moderating role of spatial configuration in
900 producing dominance asymmetry. This susceptibility of dominance asymmetry to stimulus presentation

901 is consistent with evidence from prior work on the effect of presentation formats on AE, as reviewed by
902 [Spektor et al. \(2021\)](#), tested by [Cataldo and Cohen \(2018, 2019\)](#); [Evans et al. \(2019\)](#), and more recently by
903 [Hasan et al. \(2025\)](#). Whether this sensitivity of asymmetric dominance, and hence the attraction effect,
904 to the presentation format generalizes to other perceptual stimuli beyond rectangles remains a fruitful
905 direction for future research.

906 Third, although we inferred attentional weighting from choice and subjective difficulty ratings, we did not
907 directly measure attentional allocation. Process-tracing approaches such as eye-tracking or mouse-tracking
908 would provide more direct evidence about how participants allocate attention and engage in the comparison
909 processes that drive the attraction effect. Previous research demonstrates that eye-tracking can illuminate
910 the mechanisms underlying context effects in multiattribute choice, especially by revealing how attention
911 is distributed between choice alternatives ([Noguchi and Stewart, 2014](#); [Marini et al., 2020](#); [Molter et al.,
912 2022](#); [Cataldo and Cohen, 2019](#)). For instance, [Noguchi and Stewart \(2014\)](#) and [Marini et al. \(2020\)](#) have
913 shown that shifts in gaze patterns reflect comparative processes pivotal to the emergence (or suppression) of
914 decoy effects, while [Molter et al. \(2022\)](#) demonstrate that gaze-dependent evidence accumulation predicts
915 behavioral responses in multi-alternative choice. Incorporating such measures in future work would not only
916 clarify the attentional dynamics involved in perceptual attraction effects but would also help to distinguish
917 between competing process models.

918 Fourth, the present work focused on pairwise asymmetric-dominance boundary conditions and presenta-
919 tion layout manipulations, but other situational constraints may also play a role. Factors such as decision
920 time pressure, cognitive load could interact with the process responsible for dominance asymmetry, shaping
921 the emergence and strength of AE. Prior research has demonstrated that time constraints may reduce
922 the incidence or magnitude of context effects, including the attraction effect, by limiting the opportunity
923 for deliberation and comparative processing ([Spektor et al., 2021](#); [Pettibone, 2012](#)). Similarly, increased
924 cognitive load might disrupt the necessary information integration, potentially attenuating or altering
925 context effects (see, e.g., [Spektor et al. \(2021\)](#)). Examining the roles of these factors and their interactions
926 would further refine the boundary conditions identified in this study.

927 Fifth, we did not include dedicated pairwise Target-Competitor (T-C) trials in Experiment 1 to empirically
928 verify the assumed equivalence between core alternatives. Although T and C were designed to be equal on
929 respective criterion values, this equivalence was achieved by design rather than confirmed behaviorally.
930 Prior attraction effect research typically establishes such equivalence by design to ensure that any shift in
931 relative choice share arises from the inclusion of the decoy rather than pre-existing bias between the core
932 options. Future studies should explicitly incorporate T-C pairwise comparisons to validate this assumption
933 and strengthen interpretations regarding asymmetric dominance and the robustness of the attraction effect
934 under different stimulus types.

935 Yet, another limitation of the present work is that our two stimulus sets—rectangles and star-shaped
936 figures—differ not only in their perceptual appearance but also in the specific judgment task associated
937 with each. For rectangles, participants identified the item with the greatest area, whereas for stars, they
938 judged the item requiring the least sand to complete a square. These differences raise the possibility that
939 task-related demands or stimulus complexity may modulate the observed attraction effect. However, both
940 stimulus sets were carefully designed such that variation was restricted to two orthogonal attributes, and
941 the decoy manipulations were defined within the same attribute-based framework. We therefore interpret
942 the present findings as evidence that the principle demonstrated here is not exclusive to one stimulus type
943 or task, while recognizing that a broader range of stimuli and tasks will need to be examined in future work
944 to establish the generality of the claims.

945 Seventh, the generalizability of attraction effects to naturalistic decision contexts remains an important
946 open question ([Frederick et al., 2014](#); [Huber et al., 2014](#); [Trendl et al., 2021](#)). Our framework suggests
947 that the absence of asymmetric dominance—rather than stimulus type itself—may explain null effects
948 in naturalistic contexts. Future research should systematically construct naturalistic choice sets in which
949 genuine item-level dominance asymmetry is clearly established, to determine whether attraction effects
950 can emerge in ecologically valid decision environments and to further refine boundary conditions across
951 diverse stimulus domains.

952 Eighth, our present findings are restricted to visual perceptual choice with controlled dominance asymme-
953 try, leaving open the question of whether the attraction effect generalizes to other sensory modalities such
954 as auditory or tactile domains. To guide this endeavor, the computational and neurocognitive framework

955 articulated by [Busemeyer et al. \(2019\)](#) is especially relevant: their sequential sampling models propose
956 that context effects such as the attraction effect arise from dynamic processes involving shifting attentional
957 focus, lateral inhibition among competing options, and real-time integration of attribute comparisons—core
958 computations implemented through a distributed network of prefrontal and parietal regions. This framework
959 predicts not only where in the brain such effects may emerge, but how their magnitude and neural signatures
960 will depend on stimulus structure and deliberation time, offering specific, testable hypotheses for new
961 domains. Although this account suggests the possibility of domain-general mechanisms for context effects
962 ([Pisauro et al., 2017](#); [Levy and Glimcher, 2012](#); [Philiastides et al., 2011](#)), recent findings demonstrate
963 modality-specific effects in the timing and locus of irrelevant information processing ([Li et al., 2024](#)).
964 Thus, future studies must carefully design behavioral and neuroimaging paradigms tailored to each sensory
965 modality, to empirically test whether dominance asymmetry produces attraction effects and whether their
966 neural basis aligns with Busemeyer et al.'s process-level predictions across different domains.

967 A related and broader theoretical issue concerns the interpretation of attraction effects within the neuro-
968 science of decision-making. Historically, the attraction effect has been viewed as a violation of rational
969 value computation by economic models of choice. However, recent critiques ([Hayden and Niv, 2021](#))
970 contend that regions such as orbitofrontal cortex encode structured comparative signals rather than single
971 value representations, suggesting that so-called “irrational” context effects may instead be lawful outcomes
972 of the way brains process multi-attribute information. Our dominance asymmetry framework provides
973 a bridge between these perspectives, proposing that attraction effects and preference reversals reflect
974 structural features of comparative processing rather than failures of value encoding per se. Neuroimaging
975 studies that rigorously manipulate dominance asymmetry, coupled with process-tracing of comparative
976 attention and attribute integration, will be necessary to establish whether attraction effects are best explained
977 by competitive structural mechanisms or truly signal limits to rational economic computation.

978 Together, these limitations and future directions highlight how specifying effective stimulus properties,
979 testing the generalizability of dominance asymmetry beyond traditional visual domains, incorporating richer
980 process-tracing and neuroimaging measures, and broadening the scope across sensory modalities, tasks,
981 and theoretical frameworks can advance our understanding of when and why the attraction effect emerges.
982 By integrating behavioral, computational, and neural approaches, future research will be positioned to
983 clarify whether the attraction effect reflects deep structural mechanisms of comparative decision-making or
984 signals fundamental constraints on value-based rationality.

985 6.5 Conclusion

986 Across four experiments, we resolved apparent contradictions in the literature by demonstrating that
987 the attraction effect reliably emerges in perceptual decision-making when proper conditions of item-wise
988 asymmetric dominance are met. These findings refine theoretical accounts of AE by highlighting the central
989 role of pairwise comparison processes, while also providing methodological guidance for how to design
990 and validate effective stimuli. More broadly, they support a unified framework in which the attraction effect
991 reflects fundamental properties of human information processing that generalize from consumer choices to
992 perceptual judgments. By establishing clear boundary conditions, our work clarifies when AE should and
993 should not be expected, offering a stronger foundation for future investigations of this robust but sometimes
994 elusive decision bias.

CONFLICT OF INTEREST STATEMENT

995 The authors declare that the research was conducted in the absence of any commercial or financial
996 relationships that could be construed as a potential conflict of interest.

ETHICS STATEMENT

997 All experiments were approved by the Institute Ethics Committee at Indian Institute of Technology Kanpur,
998 India (IITK/IEC/2023-24/II/36). Participants provided informed consent before participation and received
999 compensation for their time.

AUTHOR CONTRIBUTIONS

1000 **TR**: Conceptualization, Data curation, Formal analysis, Methodology, Software, Validation, Visualization,
1001 Writing – original draft, Writing – review & editing.

1002 **NaS**: Methodology, Supervision, Validation, Visualization, Writing – original draft, Writing – review &
1003 editing.

1004 **NiS**: Data curation, Investigation, Methodology, Supervision, Validation, Visualization, Writing – original
1005 draft, Writing – review & editing.

FUNDING

1006 No funds, grants, or other support were received for conducting this study.

DATA AVAILABILITY STATEMENT

1007 Stimulus files, raw data, and analysis code for Experiment 1, Experiment 2, Experiment 3, and Experiment
1008 4 are made available online at [OSF](#). Experiment 1 was preregistered, and the preregistration is available at
1009 [OSF](#).

REFERENCES

- 1010 Banerjee, P., Hayes, W. M., Chatterjee, P., Masters, T., Mishra, S., and Wedell, D. H. (2024a). Factors that
1011 promote the repulsion effect in preferential choice. *Judgment and Decision Making* 19, e11
- 1012 Banerjee, P., Rakshit, K., Mishra, S., and Masters, T. (2024b). Attribute ratings and their impact on
1013 attraction and compromise effects. *Marketing Letters* 35, 439–450
- 1014 Bateson, M., Healy, S. D., and Hurly, T. A. (2003). Context-dependent foraging decisions in rufous
1015 hummingbirds. *Proceedings of the Royal Society of London. Series B: Biological Sciences* 270,
1016 1271–1276
- 1017 Bhatia, S. (2013). Associations and the accumulation of preference. *Psychological review* 120, 522
- 1018 Busemeyer, J. R., Gluth, S., Rieskamp, J., and Turner, B. M. (2019). Cognitive and neural bases of
1019 multi-attribute, multi-alternative, value-based decisions. *Trends in cognitive sciences* 23, 251–263
- 1020 Cataldo, A. M. and Cohen, A. L. (2018). Reversing the similarity effect: The effect of presentation format.
1021 *Cognition* 175, 141–156
- 1022 Cataldo, A. M. and Cohen, A. L. (2019). The comparison process as an account of variation in the
1023 attraction, compromise, and similarity effects. *Psychonomic Bulletin & Review* 26, 934–942
- 1024 Chen, Z., Humphries, A., and Cave, K. R. (2019). Location-specific orientation set is independent of the
1025 horizontal benefit with or without object boundaries. *Vision* 3, 30
- 1026 Choplin, J. M. and Hummel, J. E. (2005). Comparison-induced decoy effects. *Memory & cognition* 33,
1027 332–343
- 1028 Devine, S., Goulding, J., Harvey, J., Skatova, A., and Otto, A. R. (2025). How decoy options ferment
1029 choice biases in real-world consumer decision-making. *npj Science of Learning* 10, 60
- 1030 Dumbalska, T., Li, V., Tsetsos, K., and Summerfield, C. (2020). A map of decoy influence in human
1031 multialternative choice. *Proceedings of the National Academy of Sciences* 117, 25169–25178
- 1032 Evans, N. J., Holmes, W. R., Dasari, A., and Trueblood, J. S. (2021). The impact of presentation order on
1033 attraction and repulsion effects in decision-making. *Decision* 8, 36
- 1034 Evans, N. J., Holmes, W. R., and Trueblood, J. S. (2019). Response-time data provide critical constraints
1035 on dynamic models of multi-alternative, multi-attribute choice. *Psychonomic Bulletin & Review* 26,
1036 901–933
- 1037 Farmer, G. D., Warren, P. A., El-Deredy, W., and Howes, A. (2017). The effect of expected value on
1038 attraction effect preference reversals. *Journal of Behavioral Decision Making* 30, 785–793
- 1039 Frederick, S., Lee, L., and Baskin, E. (2014). The limits of attraction. *Journal of Marketing Research* 51,
1040 487–507
- 1041 Hasan, E., Liu, Y., Owens, N., and Trueblood, J. S. (2025). A registered report on presentation factors that
1042 influence the attraction effect. *Judgment and Decision Making* 20, e6
- 1043 Hayden, B. Y. and Niv, Y. (2021). The case against economic values in the orbitofrontal cortex (or anywhere
1044 else in the brain). *Behavioral Neuroscience* 135, 192

- 1045 Hayes, W. M., Holmes, W. R., and Trueblood, J. S. (2024). Attribute commensurability and context effects
1046 in preferential choice. *Psychonomic Bulletin & Review*, 1–12
- 1047 Helgadóttir, A. (2015). *Asymmetric dominance effect in choice for others*. Ph.D. thesis, University of
1048 Iceland
- 1049 Huber, J., Payne, J. W., and Puto, C. (1982). Adding asymmetrically dominated alternatives: Violations of
1050 regularity and the similarity hypothesis. *Journal of Consumer Research*
- 1051 Huber, J., Payne, J. W., and Puto, C. P. (2014). Let's be honest about the attraction effect. *Journal of*
1052 *Marketing Research* 51, 520–525
- 1053 Kaptein, M. C., Van Emden, R., and Iannuzzi, D. (2016). Tracking the decoy: maximizing the decoy effect
1054 through sequential experimentation. *Palgrave Communications* 2, 16082. doi:10.1057/palcomms.2016.
1055 82
- 1056 Katsimpokis, D., Fontanesi, L., and Rieskamp, J. (2022). A robust Bayesian test for identifying
1057 context effects in multiattribute decision-making. *Psychonomic Bulletin & Review* doi:10.3758/
1058 s13423-022-02157-2
- 1059 Kornienko, T. (2013). *Nature's measuring tape: A cognitive basis for adaptive utility*. Tech. rep., Working
1060 paper, University of Edinburgh.[CYO]
- 1061 Latty, T. and Beekman, M. (2011). Irrational decision-making in an amoeboid organism: transitivity and
1062 context-dependent preferences. *Proceedings of the Royal Society B: Biological Sciences* 278, 307–312
- 1063 Lea, A. M. and Ryan, M. J. (2015). Irrationality in mate choice revealed by túngara frogs. *Science* 349,
1064 964–966
- 1065 Levy, D. J. and Glimcher, P. W. (2012). The root of all value: a neural common currency for choice.
1066 *Current opinion in neurobiology* 22, 1027–1038
- 1067 Li, J., Hua, L., and Deng, S. W. (2024). Modality-specific impacts of distractors on visual and audi-
1068 tory categorical decision-making: an evidence accumulation perspective. *Frontiers in Psychology* 15,
1069 1380196
- 1070 Luce, R. D. (1957). A theory of individual choice behavior
- 1071 Luce, R. D. (1977). The choice axiom after twenty years. *Journal of Mathematical Psychology* 15,
1072 215–233. doi:10.1016/0022-2496(77)90032-3
- 1073 Marini, M., Ansani, A., and Paglieri, F. (2020). Attraction comes from many sources: Attentional and
1074 comparative processes in decoy effects. *Judgment and decision making* 15, 704–726
- 1075 Miller, J. (2024). How many participants? how many trials? maximizing the power of reaction time studies.
1076 *Behavior research methods* 56, 2398–2421
- 1077 Molter, F., Thomas, A. W., Huettel, S. A., Heekeren, H. R., and Mohr, P. N. (2022). Gaze-dependent
1078 evidence accumulation predicts multi-alternative risky choice behaviour. *PLoS computational biology*
1079 18, e1010283
- 1080 Noguchi, T. and Stewart, N. (2014). In the attraction, compromise, and similarity effects, alternatives are
1081 repeatedly compared in pairs on single dimensions. *Cognition* 132, 44–56
- 1082 Noguchi, T. and Stewart, N. (2018). Multialternative decision by sampling: A model of decision making
1083 constrained by process data. *Psychological review* 125, 512
- 1084 Parrish, A. E., Evans, T. A., and Beran, M. J. (2015). Rhesus macaques (*macaca mulatta*) exhibit the decoy
1085 effect in a perceptual discrimination task. *Attention, Perception, & Psychophysics* 77, 1715–1725
- 1086 Pettibone, J. C. (2012). Testing the effect of time pressure on asymmetric dominance and compromise
1087 decoys in choice. *Judgment and Decision making* 7, 513–521
- 1088 Piliastides, M. G., Aukstulewicz, R., Heekeren, H. R., and Blankenburg, F. (2011). Causal role of
1089 dorsolateral prefrontal cortex in human perceptual decision making. *Current biology* 21, 980–983
- 1090 Pisauro, M. A., Fouragnan, E., Retzler, C., and Piliastides, M. G. (2017). Neural correlates of evidence
1091 accumulation during value-based decisions revealed via simultaneous eeg-fMRI. *Nature communications*
1092 8, 15808
- 1093 Roe, R. M., Busemeyer, J. R., and Townsend, J. T. (2001). Multialternative decision field theory: A
1094 dynamic connectionist model of decision making. *Psychological review* 108, 370
- 1095 Ronayne, D. and Brown, G. D. (2017). Multi-attribute decision by sampling: An account of the attraction,
1096 compromise and similarity effects. *Journal of Mathematical Psychology* 81, 11–27
- 1097 Russo, J. E. and Doshier, B. A. (1983). Strategies for multiattribute binary choice. *Journal of Experimental*
1098 *Psychology: Learning, Memory, and Cognition* 9, 676
- 1099 Scarpi, D. (2011). The impact of phantom decoys on choices in cats. *Animal Cognition* 14, 127–136

- 1100 Shafir, S., Waite, T. A., and Smith, B. H. (2002). Context-dependent violations of rational choice in
1101 honeybees (*apis mellifera*) and gray jays (*perisoreus canadensis*). *Behavioral Ecology and Sociobiology*
1102 51, 180–187
- 1103 Spektor, M. S., Bhatia, S., and Gluth, S. (2021). The elusiveness of context effects in decision making.
1104 *Trends in Cognitive Sciences* 25, 843–854. doi:10.1016/j.tics.2021.07.011
- 1105 Spektor, M. S., Kellen, D., and Hotaling, J. M. (2018). When the good looks bad: An experimental
1106 exploration of the repulsion effect. *Psychological science* 29, 1309–1320. Publisher: Sage Publications
1107 Sage CA: Los Angeles, CA
- 1108 Spektor, M. S., Kellen, D., and Klauer, K. C. (2022). The repulsion effect in preferential choice and its
1109 relation to perceptual choice. *Cognition* 225, 105164. Publisher: Elsevier
- 1110 Srivastava, N. and Schrater, P. (2015). Learning what to want: context-sensitive preference learning. *PloS*
1111 *one* 10, e0141129
- 1112 Trendl, A., Stewart, N., and Mullett, T. L. (2021). A zero attraction effect in naturalistic choice. *Decision*
1113 8, 55
- 1114 Trueblood, J., Liu, Y., Murrow, M., Hayes, W., and Holmes, W. (2022). Attentional dynamics explain the
1115 elusive nature of context effects [psyarxiv preprint]
- 1116 Trueblood, J. S. (2012). Multialternative context effects obtained using an inference task. *Psychonomic*
1117 *bulletin & review* 19, 962–968
- 1118 Trueblood, J. S., Brown, S. D., and Heathcote, A. (2014). The multiattribute linear ballistic accumulator
1119 model of context effects in multialternative choice. *Psychological review* 121, 179
- 1120 Trueblood, J. S., Brown, S. D., Heathcote, A., and Busemeyer, J. R. (2013). Not just for consumers:
1121 Context effects are fundamental to decision making. *Psychological science* 24, 901–908
- 1122 Tsal, Y. (1989). Attending to horizontal, diagonal, and vertical positions in space. *Bulletin of the*
1123 *Psychonomic Society* 27, 133–134
- 1124 Turner, B. M., Schley, D. R., Muller, C., and Tsetsos, K. (2018). Competing theories of multialternative,
1125 multiattribute preferential choice. *Psychological review* 125, 329
- 1126 Tversky, A. (1972). *Elimination by aspects: A theory of choice.*, vol. 79 (Psychological review)
- 1127 Usher, M. and McClelland, J. L. (2004). Loss aversion and inhibition in dynamical models of
1128 multialternative choice. *Psychological review* 111, 757
- 1129 Vlaev, I., Chater, N., Stewart, N., and Brown, G. D. (2011). Does the brain calculate value? *Trends in*
1130 *cognitive sciences* 15, 546–554
- 1131 Walasek, L. and Brown, G. D. (2023). Incomparability and incommensurability in choice: no common
1132 currency of value? *Perspectives on Psychological Science* , 17456916231192828
- 1133 Wedell, D. H. (1991). Distinguishing among models of contextually induced preference reversals. *Journal*
1134 *of Experimental Psychology: Learning, Memory, and Cognition* doi:10.1037/0278-7393.17.4.767
- 1135 Wollschläger, L. M. and Diederich, A. (2012). The 2 n-ary choice tree model for n-alternative preferential
1136 choice. *Frontiers in psychology* 3, 189
- 1137 Yang, S. and Lynn, M. (2014). More evidence challenging the robustness and usefulness of the attraction
1138 effect. *Journal of Marketing Research* 51, 508–513
- 1139 Zhen, S. and Yu, R. (2016). The development of the asymmetrically dominated decoy effect in young
1140 children. *Scientific reports* 6, 22678
- 1141 Žofák, P. (2016). *The asymmetric dominance effect: Three-attribute phantom alternative at play*. Bachelor's
1142 thesis, Univerzita Karlova, Fakulta sociálních věd

Supplementary Material

1 CRITERION VALUE COMPUTATION FOR STIMULI

Rectangle Stimuli

For rectangle stimuli, the criterion value was defined as the area:

$$\text{Criterion value}_{\text{rectangle}} = w \times H$$

where w denotes the width and H the height of the rectangle. Both attributes were systematically varied to create the required ranges of target–decoy distances.

Quantitatively, the target–decoy distance (TD_dist%) for rectangles had a mean of 11.12% (SD = 2.13%), ranging from 7.23% to 14.54%.

Star Stimuli

1.0.0.1 Construction and Geometry

Star-shaped stimuli were derived from a base rectangle of width w and height H , with four inward-facing isosceles triangles (each of height d) removed—two from the vertical sides (base H , height d), two from the horizontal sides (base w , height d). This produces a star-like silhouette (see Supplementary Figure [S1](#)).

1.0.0.2 Criterion Value Formula (Stepwise Derivation)

The criterion value for the star equals the extra area needed to fill the star shape into a perfect square (of side H):

1. **Area of the square:**

$$A_{\text{square}} = H^2$$

2. **Area of the base rectangle:**

$$A_{\text{rect}} = w \times H$$

3. **Total area removed by triangles:**

$$A_{\text{removed}} = 2 \left(\frac{1}{2} H d \right) + 2 \left(\frac{1}{2} w d \right) = H d + w d$$

4. **Area of the star:**

$$A_{\text{star}} = w H - (H d + w d) = w H - H d - w d$$

5. **Criterion value:**

$$\text{CV}_{\text{star}} = H^2 - (w H - H d - w d) = H^2 - w H + H d + w d$$

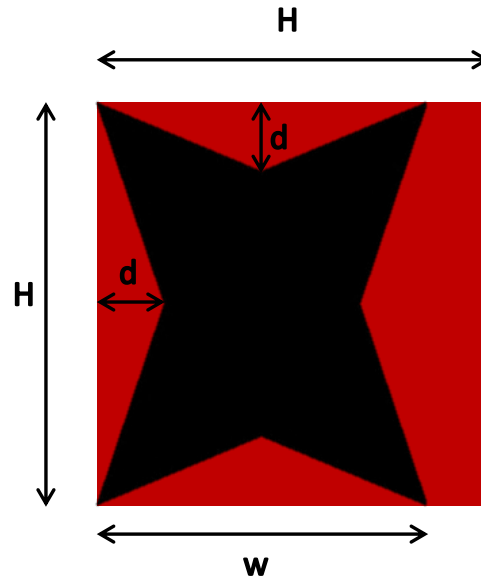


Figure S1. Example of a star-shaped stimulus derived from a rectangle (width w , height H) with four triangles (height d) removed. Figure is annotated to show w , H , d , and the extra area (criterion value) required to complete to a square. The filled-in square and removed triangles are depicted, with all parameters clearly labeled.

$$\text{Criterion value}_{\text{star}} = H^2 - wH + Hd + wd$$

Quantitatively, the target–decoy distance for stars (TD_dist%) had a mean of 13.97% (SD = 2.10%), ranging from 10.53% to 16.91%.

1.0.0.3 Practice Session: Comprehension of Criterion Value

A feedback-based practice session ensured participants understood the computation: participants could click star shapes to see them filled to a perfect square, with extra area highlighted and a numerical value displayed underneath. This provided intuitive feedback on the “extra sand” concept (criterion value). No special practice was needed for rectangles.

1.0.0.4 Comparability and Range

Both stimuli types are governed by two orthogonal, independently varied attributes. The stimulus file with all parameter values is available in the OSF repository.

2 SENSITIVITY ANALYSIS FOR EXPERIMENT 1

In attraction-effect paradigms, the *Target–Decoy distance percentage* ($TD_dist\%$)—that is, the relative difference between the target and decoy on the relevant criterion dimension—should ideally have similar distributions across stimulus types to allow for a fair comparison of context effects. Matching $TD_dist\%$ ensures that any observed behavioral differences are not driven by differences in relative discriminability but instead reflect genuine psychological or perceptual effects.

In practice, however, perfect alignment of $TD_dist\%$ distributions is often difficult to achieve when stimuli differ geometrically or when parametric constraints interact nonlinearly, as in the case of the star stimuli. The nonlinear dependencies introduced by the star's criterion value make it infeasible to ensure an exact per-trial match with the rectangular stimuli without generating visually implausible or perceptually imbalanced shapes. Nevertheless, our goal was to create broadly comparable ranges across both stimulus types.

Upon closer inspection, we observed a modest but statistically significant difference in the $TD_dist\%$ distributions between rectangles ($M \approx 11.5\%$) and stars ($M \approx 14.0\%$) in our stimulus set (see Fig S2). This discrepancy arose from practical constraints in stimulus generation and was not intentional. Importantly, the chosen $TD_dist\%$ ranges are consistent with values commonly used in previous attraction-effect studies to manipulate discriminability (e.g., (Wedell, 1991; Farmer et al., 2017; Spektor et al., 2018))

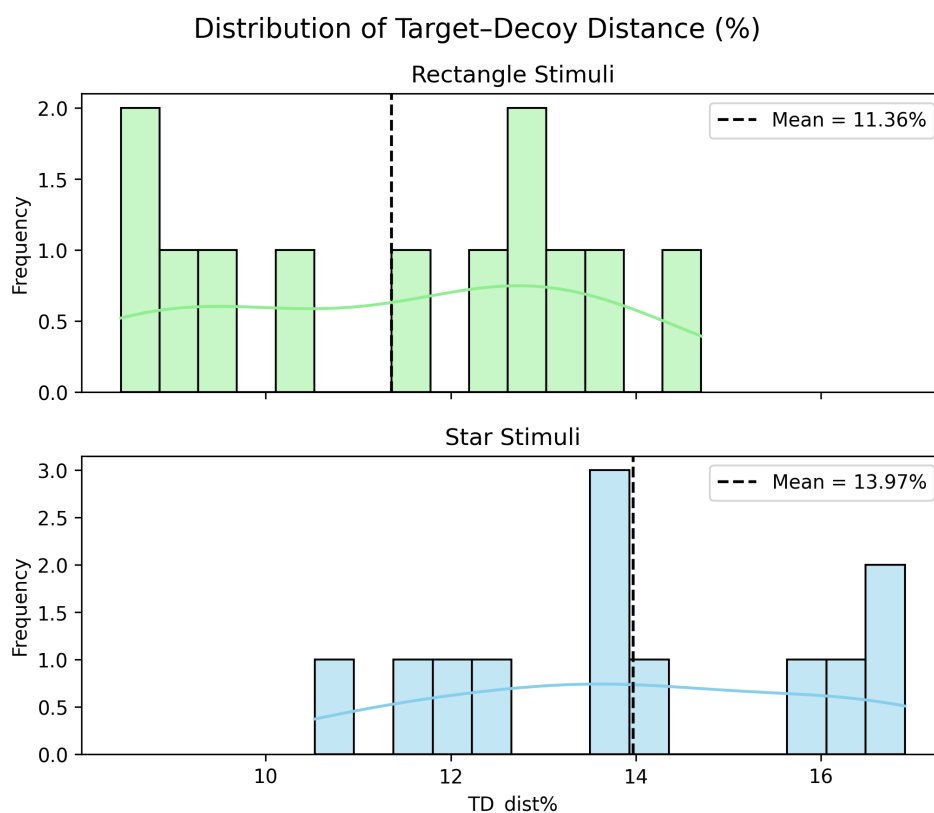


Figure S2. Distribution of target–decoy distance percentages ($TD_{dist}\%$) for all rectangle and star stimuli included in the experiment. The distributions reveal a modest but statistically significant difference in the average $TD_dist\%$ between rectangles ($M \approx 11.5\%$) and stars ($M \approx 14.0\%$).

To directly address potential concerns that this difference might have influenced the main results, we conducted a *sensitivity analysis* restricted to the subset of trials for which the TD_{dist}% ranges overlapped for both rectangles and stars, calculated separately for each participant. While the original dataset comprised 2,817 trials, the filtered subset included 2,451 trials (approximately 87% of the total).

A Wilcoxon signed-rank test comparing the TD_{dist}% distributions across stimulus types revealed no significant difference after filtering ($W = 790.00$, $p = 0.26$). Crucially, the main and interaction effects for accuracy, reaction time, and difficulty ratings all remained robust and statistically significant, with effect sizes and significance levels nearly identical to those obtained from the full dataset (see Supplementary Table S1 and Figure S3).

Table S1. Repeated measures ANOVA results for accuracy, reaction time, and difficulty rating using only trials in the overlapping TD_{dist}% range for both rectangles and stars (sensitivity analysis). Each row reports the F value, p value, and partial eta squared (η_p^2) for the corresponding main effect or interaction.

Factor	$F(1, 60)$	p	η_p^2
Accuracy			
Stimulus type	24.48	< .001	.29
Pair	79.39	< .001	.57
Stimulus type \times Pair	7.73	.007	.11
Reaction Time			
Stimulus type	24.22	< .001	.29
Pair	8.07	.006	.12
Stimulus type \times Pair	4.03	.049	.06
Difficulty Rating			
Stimulus type	3.70	.059	.06
Pair	19.27	< .001	.24
Stimulus type \times Pair	6.96	.011	.10

Pairwise post hoc t -tests (sensitivity analysis): Using only trials in the overlapping TD_{dist}% range, the accuracy difference between pairs remained highly significant for the star stimuli ($t(60) = 7.13$, $p < .001$, Cohen's $d = 1.031$, mean difference = 0.181, SD = 0.199), mirroring the unfiltered analysis. For rectangle stimuli, the pairwise difference also remained robust and significant ($t(60) = 4.86$, $p < .001$, Cohen's $d = 0.659$, mean difference = 0.091, SD = 0.146).

These findings confirm that the reported effects are not artifacts of differences in TD_{dist}% distributions but instead reflect genuine underlying variations in attentional and perceptual processing between the two stimulus types.

3 BASELINE PREFERENCE CHECK IN EXPERIMENT 1

To ensure that the observed dominance asymmetry in Experiment 1 was not confounded by a baseline preference for either the wide (W) or narrow (N) core option, we conducted a generalized linear mixed-effects model (GLMM) analysis. The model predicted trial-level accuracy (correct/incorrect) with fixed effects of pair type (target-decoy [TD] vs. competitor-decoy [CD]), target type (W vs. N), their interaction, and stimulus type (rectangle vs. star). A random intercept for participant was included to account for repeated measures.

3.1 Model specification

The GLMM was fitted using the binomial family with a logit link. The formula in R notation was:

$$\text{correct} \sim \text{pair} * \text{target_type} + \text{stimulus_type} + (1 | \text{userId})$$

where `correct` is a binary variable (1 = correct, 0 = incorrect), `pair` is TD or CD, `target_type` is W or N, `stimulus_type` is rectangle or star, and `userId` is the participant identifier.

The analysis included 2,809 trials from 61 participants. The random effect variance for participant intercepts was 0.45 (SD = 0.67). Model fit indices were AIC = 2,333.8 and BIC = 2,369.4.

3.2 Results

Table S2. Fixed effects estimates from the GLMM predicting accuracy in Experiment 1. Odds ratios (OR) are derived from the logistic model coefficients.

Predictor	Estimate	SE	z	p	OR
(Intercept)	1.67	0.14	11.56	< .001	5.31
Pair TD	1.15	0.16	7.10	< .001	3.15
Target type W	-0.01	0.13	-0.08	.94	0.99
Stimulus type star	-0.66	0.11	-6.06	< .001	0.52
Pair TD × Target type W	-0.14	0.22	-0.63	.53	0.87

Note. SE = standard error; OR = odds ratio.

As shown in Table [S2](#), the main effect of pair type was significant, with higher accuracy for TD pairs than for CD pairs (odds ratio = 3.15). There was no significant main effect of target type (W vs. N; $p = .94$), indicating that participants did not exhibit an inherent bias toward either core option. The interaction between pair type and target type was also nonsignificant ($p = .53$), suggesting that the accuracy advantage for TD pairs was consistent regardless of target type.

These results confirm that the dominance asymmetry observed in Experiment 1 cannot be attributed to a baseline preference for either the wide or narrow core option. The effect of pair type on accuracy was robust and stable across target conditions, reinforcing the validity of the main experimental findings.

4 PILOT STUDY AND STIMULUS ADJUSTMENT PROCEDURE IN EXPERIMENT 2

We conducted a pilot study prior to Experiment 2, employing triplet sets typical of attraction effect designs (Target, Competitor, Decoy) with attributes systematically varied. The pilot revealed a moderate bias in favor of one core option (typically the wider star) in the final triplet choice.

In Experiment 1, our design focused exclusively on pairwise Target–Decoy (TD) and Competitor–Decoy (CD) comparisons, omitting dedicated Target–Competitor (T–C) trials. While core options were carefully designed to be equivalent on the relevant criterion dimension (see Section 6.4, Limitations and Future Directions, main text), formal behavioral verification of T–C equivalence was not performed. Although our GLMM analyses found no significant target type effects under pairwise conditions in Experiment 1, the pilot study suggested that triplet presentations might amplify even subtle preference tendencies, necessitating empirical calibration in Experiment 2.

To ensure that such a bias did not confound the measurement of the attraction effect or reduce the effect sizes, we implemented a targeted stimulus adjustment. Specifically, the width of the narrower star shape (w_2) was increased by 10 pixels for Experiment 2. This correction was calibrated to restore choice parity between core shapes within triplet sets, supporting the integrity of the subsequent analyses.

A graphical depiction of these adjustments is presented in Supplementary Figure S4. It illustrates the core star stimuli in 2D attribute space, visually depicting the 10-pixel increase in w_2 applied for Experiment 2. The figure provides a clear visual comparison of the core item configurations across experimental designs.

In summary, our pilot-based adjustments and rigorous baseline checks across designs strengthen the validity and interpretability of context-dependent choice effects, while also highlighting the importance of direct core alternative comparisons in future studies.

5 REPLICATION OF SPEKTOR ET AL. (2018) AND REANALYSIS OF SPEKTOR ET AL. (2022)

Rationale for Replication

In our study, the central thesis is that asymmetric dominance of the decoy is a necessary precondition for the emergence of the attraction effect in triplet choice sets. Given that our Experiment 1 revealed only weak asymmetric dominance of decoys for rectangles in pairwise comparisons, we predicted that such stimuli should not generate a robust repulsion effect, but rather a reduced or null attraction effect.

Interestingly, the same rectangular stimuli have been shown to produce both positive attraction effects—when arranged in a linear display layout (as in Trueblood et al. (2013) and Experiment 4a in Spektor et al. (2018))—and negative effects, as reported in Experiments 1, 2, 3, and 4b of Spektor et al. (2018) when presented in a triangular display layout. Moreover, other perceptual stimuli, such as bars, have also produced negative attraction (repulsion) effects in triangular layouts (Spektor et al., 2022).

Our analysis of both Spektor et al. (2018) and Spektor et al. (2022) revealed a methodological feature uncommon among attraction effect studies. Typically, such studies equate the two core alternatives on the decision-relevant dimension or criterion value (e.g., equal area, equal value-for-money), ensuring that any bias in choice behavior can be attributed solely to the presence of a decoy. In contrast, these two studies implemented a richer within-subject design with multiple, simultaneously manipulated factors—including correct option/larger, set type, difficulty, target, decoy type, and attribute distance. The stimuli consisted of either rectangle or bar pairs (wide-but-low and narrow-but-high), with participants asked to select the option with the highest total criterion (area or total filled length).

Crucially, the experimental designs in both studies manipulated the discriminability between core options (e.g., 3% versus 7% difference), a feature rarely included but theoretically important for understanding the strength of pre-decoy preferences.

Because the data from both studies are publicly available, it is feasible to reanalyse them to assess whether the originally reported negative attraction effects persist when all manipulations are explicitly modelled. However, given the likelihood that these manipulations interact with the underlying requirement of asymmetric dominance for the decoy, we chose instead to conduct a conceptual replication of Spektor et al. (2018)'s triangular triplet design using stimuli of comparable size.

Nonetheless, we did reanalyze the data from Spektor et al. (2022) and found that the previously reported reversed attraction effect is not robust, but rather better explained as null findings when multiple design factors are jointly modelled.

Model Specification for Reanalysis

We fitted a series of generalized linear mixed-effects models (GLMMs) using the lme4 package (Bates et al., 2015), based on data from 54,916 trials across 55 participants. The models predicted binary responses (NH = 1, WL = 0) and included random intercepts for participants. The primary predictor of interest was the *target* variable, which indicates which of the two core options (NH or WL) was designated as the target on a given trial. This variable captures the hypothesized influence of the decoy.

Candidate models included progressively more complex specifications, beginning with a null model (random intercepts only), an additive model including *larger*, *target*, *difficulty*, and *condition*, and extending to interaction models incorporating two-way and three-way interactions among these predictors. In total, fifteen models were estimated, labeled A through D3 in Table S3.

Model	Formula
A0	True_response_bin ~ 1 + (1 subject_id)
A	True_response_bin ~ larger + target + difficulty + condition + (1 subject_id)
B1	True_response_bin ~ larger * target + difficulty + condition + (1 subject_id)
B2	True_response_bin ~ larger * difficulty + target + condition + (1 subject_id)
B2_reduced	True_response_bin ~ larger * difficulty + target + (1 subject_id)
B3	True_response_bin ~ larger * condition + target + difficulty + (1 subject_id)
B4	True_response_bin ~ target * difficulty + larger + condition + (1 subject_id)
B5	True_response_bin ~ target * condition + larger + difficulty + (1 subject_id)
B6	True_response_bin ~ difficulty * condition + larger + target + (1 subject_id)
C1	True_response_bin ~ larger * target + larger * difficulty + condition + (1 subject_id)
C2	True_response_bin ~ larger * difficulty + condition * target + (1 subject_id)
C3	True_response_bin ~ larger * condition + difficulty * target + (1 subject_id)
D1	True_response_bin ~ larger * difficulty * condition + target + (1 subject_id)
D2	True_response_bin ~ larger * target * condition + difficulty + (1 subject_id)
D3	True_response_bin ~ larger * target * difficulty + condition + (1 subject_id)

Table S3. Candidate GLMER models for binary response (True_response_bin), from null (A0) to additive (A) to interactions (B1–B6, C1–C3, D1–D3).

The best-fitting model (Model D1) can be expressed as:

$$\text{logit}(P(\text{NH response})) = \beta_0 + \beta_1 \text{larger} + \beta_2 \text{difficulty} + \beta_3 \text{condition} + \beta_4 \text{target} + \beta_{5-8} \text{interactions} + u_{\text{subject}} \quad (\text{S1})$$

Expanded form (on the logit scale):

$$\begin{aligned} \text{logit}(P(Y_{ij} = 1)) = & \beta_0 + \beta_1 \text{larger}_{ij} + \beta_2 \text{difficulty}_{ij} + \beta_3 \text{condition}_{ij} + \beta_4 \text{target}_{ij} \quad (\text{S2}) \\ & + \beta_5 (\text{larger} \times \text{difficulty})_{ij} + \beta_6 (\text{larger} \times \text{condition})_{ij} + \beta_7 (\text{difficulty} \times \text{condition})_{ij} \\ & + \beta_8 (\text{larger} \times \text{difficulty} \times \text{condition})_{ij} + u_{0j}. \end{aligned}$$

Where:

- Y_{ij} : binary response for trial i from participant j , coded as 1 = NH chosen, 0 = WL chosen.

- $\text{logit}(p) = \ln\left(\frac{p}{1-p}\right)$: log-odds link function for binomial models.
- β_0 : fixed intercept (baseline log-odds when predictors are at their reference levels).
- β_1, \dots, β_4 : main effects of *larger* (which option had greater fill), *difficulty* (3% vs. 7%), *condition* (baseline vs. preferential), and *target*.
- $\beta_5, \beta_6, \beta_7$: coefficients for two-way interactions.
- β_8 : coefficient for the three-way interaction.
- $u_{0j} \sim \mathcal{N}(0, \sigma^2)$: subject-specific random intercept, capturing individual differences in baseline choice tendencies.

In R notation (using `lme4`; Bates et al. (2015)), the model was specified as:

```
True_response_bin ~ larger * difficulty * condition
                    + target + (1 | subject_id)
```

Here, `larger * difficulty * condition` expands into all main effects and their interactions up to the three-way term, `+ target` adds the fixed effect of the decoy-targeted option, and `(1 | subject_id)` specifies random intercepts per participant.

Model Comparison

Table S4 reports the AIC and BIC values for all fifteen models. Both information criteria converged in identifying Model D1 (highlighted in the table) as the preferred specification.

Table S4. Model comparison based on AIC and BIC values. The best-fitting model (D1) is highlighted.

Model	AIC	BIC
Null	74771.88	74789.70
A	61746.59	61800.07
B1	61747.69	61810.08
B2	61261.99	61324.38
B2_reduced	61278.17	61331.65
B3	61683.93	61746.32
B4	61746.17	61808.56
B5	61743.18	61805.57
B6	61748.57	61810.97
C1	61262.81	61334.12
C2	61258.78	61330.09
C3	61683.57	61754.88
D1	61187.11	61276.24
D2	61684.65	61773.78
D3	61266.01	61355.15

Results

In the best-fitting model, the fixed-effect estimate for *target* was small and not statistically significant ($\beta = 0.0335$, $p = 0.09$). By contrast, *larger*, *difficulty*, and their higher-order interactions produced reliable effects. These findings indicate that the *target* variable—central to the definition of the attraction effect—did not substantially influence choice once other design manipulations were accounted for.

This conclusion is illustrated in Figure S5, which displays the fixed-effect estimates from the best-fitting model (D1) with 95% confidence intervals. The plot shows reliable effects of *larger*, *difficulty*, and their

interactions, whereas the coefficient for *target* is small and its confidence interval overlaps zero, indicating no substantial influence of the decoy-designated option.

5.1 Conclusion

The re-analysis indicates that the reversed attraction effect reported by [Spektor et al. \(2022\)](#) is not robust once multiple design factors are simultaneously modeled. The effect of the *target* variable is best characterized as null, consistent with the absence of a reliable attraction—or repulsion—effect under bar stimuli.

6 ROBUSTNESS OF RESULTS ACROSS EXPERIMENTS

To assess the robustness of our findings, we systematically examined the effects of commonly used participant- and trial-level exclusion criteria on the primary measure of each experiment. Experiment 1 was pre-registered, providing a reference for exclusion thresholds, whereas other experiments were not. Thresholds were therefore selected based on Experiment 1 and previous literature, including the one replicated in Experiment 3 ([Spektor et al., 2018](#)).

Exclusion Criteria

Participant-level exclusion was based on catch trial accuracy. Two thresholds were considered: 0.8 (reflecting the pre-registered criterion in Experiment 1) and a more lenient 0.677, informed by prior literature ([Spektor et al., 2018](#)). Participants performing below the threshold were excluded.

Trial-level exclusion removed implausibly fast or slow responses. Trials with reaction times below 100 ms were excluded. Upper bounds included three alternatives: a fixed 20,000 ms threshold (pre-registered in Experiment 1), a fixed 8,000 ms threshold (used in prior literature), and a participant-specific threshold defined as the 75th percentile plus 1.75 times the interquartile range of each participant's RT distribution.

Robustness Analysis Approach

For each experiment and each combination of participant- and trial-level exclusion criteria, we recomputed the primary measure (relative share of target, RST, or other experiment-specific dependent variables). Frequentist analyses used one-sample t-tests against null values (0.5 for RST), with effect sizes calculated as Cohen's *d*. Bayesian analyses were conducted in R using the `BayesFactor` package to compute Bayes factors. Experiment 4 did not include catch trials.

Results

Across all four experiments, the direction and statistical significance of the primary effects were preserved under all exclusion criteria.

Tables [S5–S8](#) provide detailed results for each experiment, including sample sizes, trials retained, mean and SD of primary measures, t-values, p-values, effect sizes, and Bayes factors. Each table follows a similar layout.

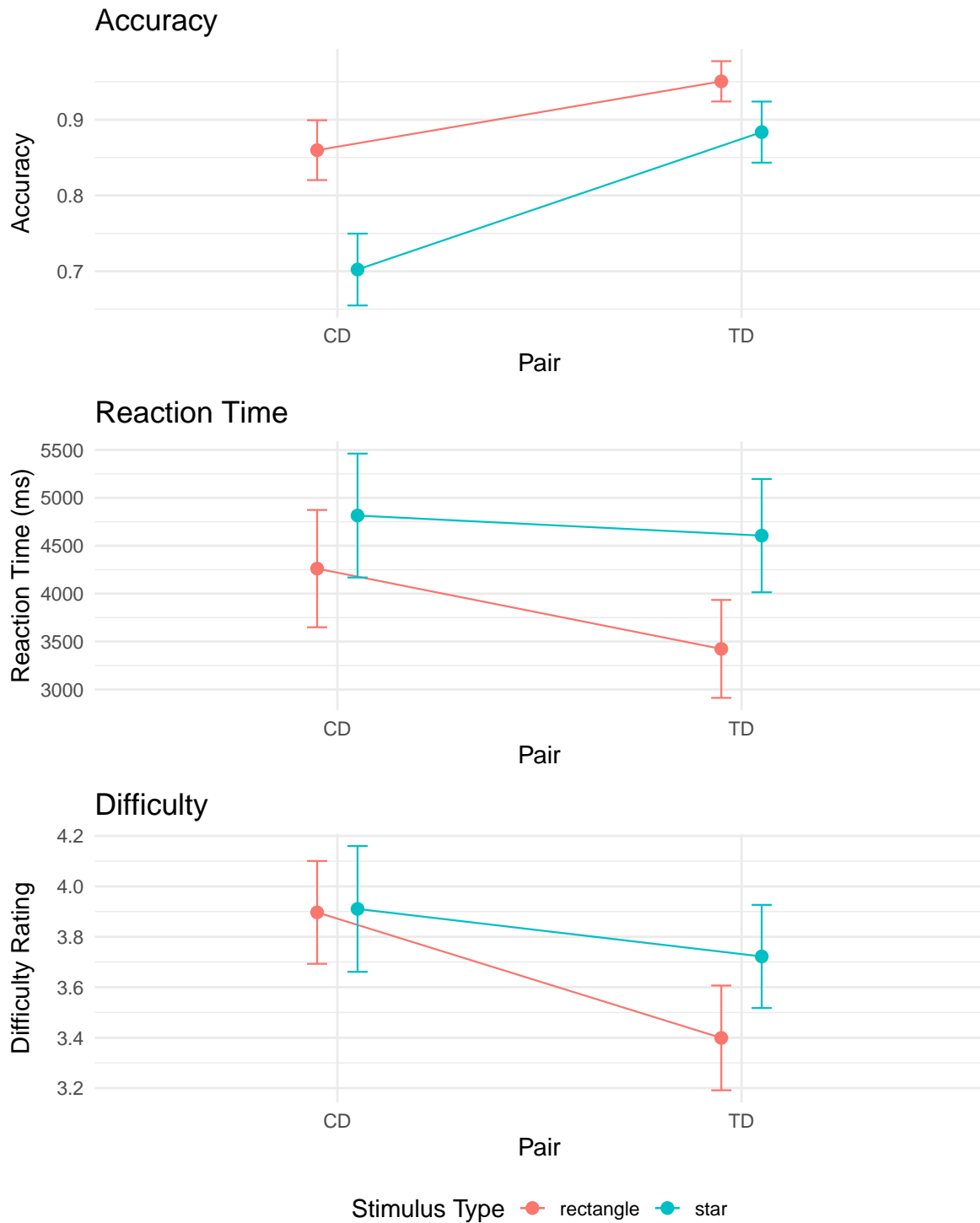


Figure S3. Interaction effects of stimulus type and pair on accuracy, reaction time, and difficulty rating, using only trials with matched overlapping $TD_{dist}\%$ ranges between rectangles and stars (sensitivity analysis). Error bars represent 95% within-subject confidence intervals.

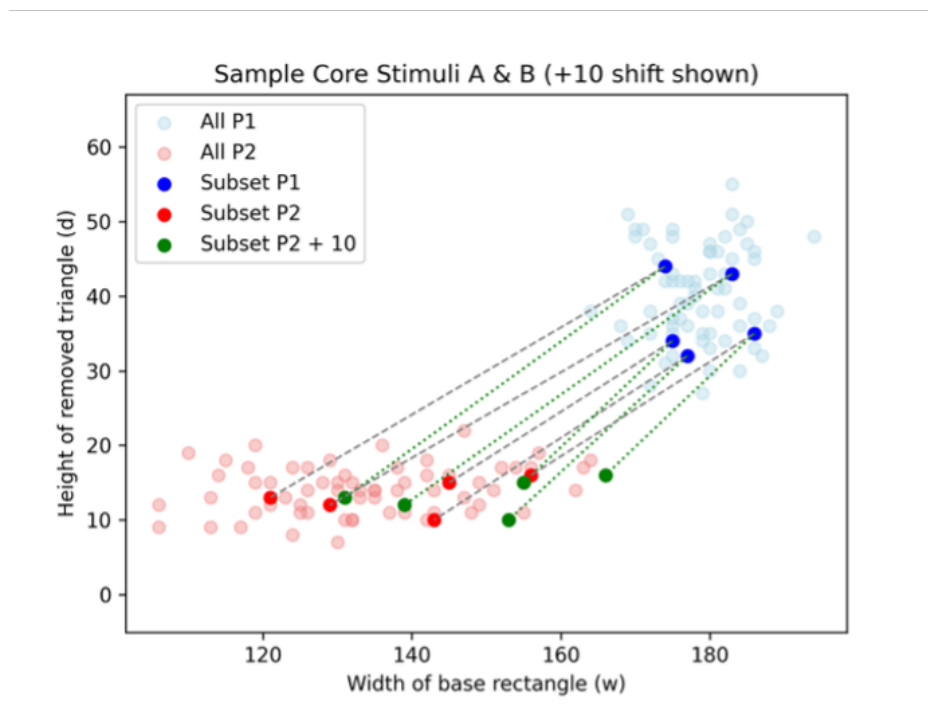


Figure S4. Core star items plotted in 2D attribute space. The adjustment of the narrower (w_2) item by 10 pixels for Experiment 2 is indicated, highlighting the bias correction relative to Experiment 1.

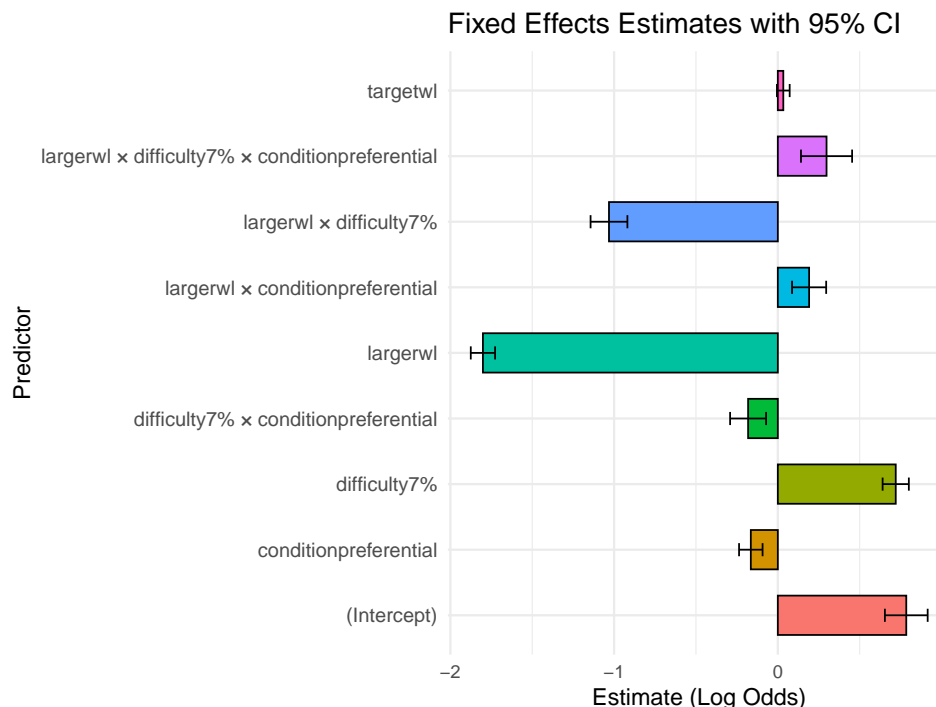


Figure S5. Estimated effects of each predictor on the probability of choosing the narrow–high (NH) option. Predictors are listed vertically; the horizontal axis shows the size and direction of each effect on the log-odds scale. Error bars are 95% confidence intervals. Effects to the right (positive) increase the chance of choosing NH; effects to the left (negative) decrease it.

Table S5. Robustness of Experiment 1 results across different participant- and trial-level exclusion criteria. **part_threshold:** participant-level catch accuracy threshold; **RT_Low / RT_Upper:** lower and upper bounds for reaction times (ms); **n_users / n_trials:** number of participants and trials before exclusion; **Trials removed%:** proportion of trials removed due to RT criteria; **effect / F / num_df / den_df / p-value / pes:** effect tested, F statistic, numerator and denominator degrees of freedom, p-value, and partial eta squared.

part_threshold	RT Low	RT Upper	n_users	n_trials	Trials removed%	effect	F	num_df	den_df	p	pes
0.8	100	20000	61	2809	0.041	stimulus_type	11.06	1	60	0.002	0.156
0.8	100	20000	61	2809	0.041	pair	75.82	1	60	< 0.001	0.558
0.8	100	20000	61	2809	0.041	stimulus_type:pair	9.81	1	60	0.003	0.140
0.8	100	15000	61	2745	0.063	stimulus_type	10.60	1	60	0.002	0.150
0.8	100	15000	61	2745	0.063	pair	64.35	1	60	< 0.001	0.517
0.8	100	15000	61	2745	0.063	stimulus_type:pair	9.15	1	60	0.004	0.132
0.8	100	10000	61	2567	0.123	stimulus_type	10.71	1	60	0.002	0.151
0.8	100	10000	61	2567	0.123	pair	56.12	1	60	< 0.001	0.483
0.8	100	10000	61	2567	0.123	stimulus_type:pair	9.44	1	60	0.003	0.136
0.8	100	8000	61	2421	0.173	stimulus_type	11.78	1	60	0.001	0.164
0.8	100	8000	61	2421	0.173	pair	51.52	1	60	< 0.001	0.462
0.8	100	8000	61	2421	0.173	stimulus_type:pair	11.41	1	60	0.001	0.160
0.677	100	20000	61	2809	0.041	stimulus_type	11.06	1	60	0.002	0.156
0.677	100	20000	61	2809	0.041	pair	75.82	1	60	< 0.001	0.558
0.677	100	20000	61	2809	0.041	stimulus_type:pair	9.81	1	60	0.003	0.140
0.677	100	15000	61	2745	0.063	stimulus_type	10.60	1	60	0.002	0.150
0.677	100	15000	61	2745	0.063	pair	64.35	1	60	< 0.001	0.517
0.677	100	15000	61	2745	0.063	stimulus_type:pair	9.15	1	60	0.004	0.132
0.677	100	10000	61	2567	0.123	stimulus_type	10.71	1	60	0.002	0.151
0.677	100	10000	61	2567	0.123	pair	56.12	1	60	< 0.001	0.483
0.677	100	10000	61	2567	0.123	stimulus_type:pair	9.44	1	60	0.003	0.136
0.677	100	8000	61	2421	0.173	stimulus_type	11.78	1	60	0.001	0.164
0.677	100	8000	61	2421	0.173	pair	51.52	1	60	< 0.001	0.462
0.677	100	8000	61	2421	0.173	stimulus_type:pair	11.41	1	60	0.001	0.160

Table S6. Robustness of Experiment 2 results across different participant- and trial-level exclusion criteria. **CatchAcc.Thres:** catch trial accuracy threshold for participant exclusion; **RT_Lower_ms / RT_Upper_ms:** lower and upper bounds for reaction times; **PSpec:** a participant-specific upper threshold, defined as the 75th percentile plus 1.75 times the interquartile range of that participant's RT distribution. **InitN / InitTrials:** initial participants and trials; **Part_N / Trials_after_Part:** after participant-level exclusion; **Final_N / Final_Trials:** after both exclusions; **Trials_Removed_%:** percentage of trials removed; **Mean_RST / Std_RST:** mean and SD of relative share of target; **t_stat / p_val / Cohen's d / BF10:** t-test statistics, p-values, effect size, and Bayes factor.

Condition	CatchAcc	RT Lower (ms)	RT Upper (ms)	Init N	Init Trials	Part N	Trials after Part	Final N	Final Trials	Trials Removed %	Mean RST	Std RST	t	p	Cohen's d	BF10
No Tech-Error Exclusion	0.80	100	20000	54	9720	52	9360	52	9048	3.33	0.54	0.05	5.73	<0.001	0.80	29268.82
No Tech-Error Exclusion	0.80	100	8000	54	9720	52	9360	52	8044	14.06	0.54	0.05	5.73	<0.001	0.79	28772.98
No Tech-Error Exclusion	0.80	100	PSpec	54	9720	52	9360	52	8832	5.64	0.54	0.05	5.60	<0.001	0.78	18659.41
No Tech-Error Exclusion	0.68	100	20000	54	9720	52	9360	52	9048	3.33	0.54	0.05	5.73	<0.001	0.80	29268.82
No Tech-Error Exclusion	0.68	100	8000	54	9720	52	9360	52	8044	14.06	0.54	0.05	5.73	<0.001	0.79	28772.98
No Tech-Error Exclusion	0.68	100	PSpec	54	9720	52	9360	52	8832	5.64	0.54	0.05	5.60	<0.001	0.78	18659.41
With Tech-Error Exclusion	0.80	100	20000	43	7740	42	7560	42	7252	4.07	0.54	0.05	4.82	<0.001	0.74	1035.96
With Tech-Error Exclusion	0.80	100	8000	43	7740	42	7560	42	6269	17.08	0.54	0.05	4.86	<0.001	0.75	1176.81
With Tech-Error Exclusion	0.80	100	PSpec	43	7740	42	7560	42	7038	6.91	0.54	0.05	4.68	<0.001	0.72	702.82
With Tech-Error Exclusion	0.68	100	20000	43	7740	42	7560	42	7252	4.07	0.54	0.05	4.82	<0.001	0.74	1035.96
With Tech-Error Exclusion	0.68	100	8000	43	7740	42	7560	42	6269	17.08	0.54	0.05	4.86	<0.001	0.75	1176.81
With Tech-Error Exclusion	0.68	100	PSpec	43	7740	42	7560	42	7038	6.91	0.54	0.05	4.68	<0.001	0.72	702.82

Table S7. Robustness of Experiment 3 results across different participant- and trial-level exclusion criteria. **CatchAcc.Thres:** catch trial accuracy threshold for participant exclusion; **RT_Lower_ms / RT_Upper_ms:** lower and upper bounds for reaction times (ms); **InitialN / InitialTrials:** number of participants and trials before exclusion; **Part_N / Trials_after_Part / Final_N / Final_Trials:** number of participants and trials after exclusions; **Trials_Removed_%:** percentage of trials removed; **Mean_RST / Std_RST:** mean and SD of relative share of target; **t_stat / p_val / Cohen's d / BF10:** t-test statistic, p-value, effect size, and Bayes factor.

Condition	CatchAcc	RT Lower (ms)	RT Upper (ms)	Initial N	Initial Trials	Part N	Trials after Part	Final N	Final Trials	Trials Removed %	Mean RST	Std RST	t	p	Cohen's d	BF10
No Tech-Error Exclusion	0.8	100	20000	76	12314	70	11342	70	11216	1.11	0.50	0.05	0.09	0.93	0.01	0.13
No Tech-Error Exclusion	0.8	100	8000	76	12314	70	11342	70	10889	3.99	0.50	0.05	0.01	0.99	0.00	0.13
No Tech-Error Exclusion	0.8	100	PSpec	76	12314	70	11342	70	10694	5.71	0.50	0.05	0.29	0.78	0.03	0.14
No Tech-Error Exclusion	0.677	100	20000	76	12314	72	11666	72	11537	1.11	0.50	0.05	0.41	0.68	0.05	0.14
No Tech-Error Exclusion	0.677	100	8000	76	12314	72	11666	72	11193	4.06	0.50	0.05	0.34	0.73	0.04	0.14
No Tech-Error Exclusion	0.677	100	PSpec	76	12314	72	11666	72	10998	5.73	0.50	0.05	0.58	0.56	0.07	0.15
With Tech-Error Exclusion	0.8	100	20000	74	11990	68	11018	68	10892	1.14	0.50	0.05	0.03	0.98	0.00	0.13
With Tech-Error Exclusion	0.8	100	8000	74	11990	68	11018	68	10566	4.10	0.50	0.05	-0.05	0.96	-0.01	0.13
With Tech-Error Exclusion	0.8	100	PSpec	74	11990	68	11018	68	10371	5.87	0.50	0.05	0.22	0.82	0.03	0.14
With Tech-Error Exclusion	0.677	100	20000	74	11990	70	11342	70	11213	1.14	0.50	0.05	0.36	0.72	0.04	0.14
With Tech-Error Exclusion	0.677	100	8000	74	11990	70	11342	70	10870	4.16	0.50	0.06	0.28	0.78	0.03	0.14
With Tech-Error Exclusion	0.677	100	PSpec	74	11990	70	11342	70	10675	5.88	0.50	0.06	0.52	0.60	0.06	0.15

Table S8. Robustness of Experiment 4 difficulty ratings across different trial-level RT exclusion criteria. **RT_Low / RT_Upper:** lower and upper bounds for reaction times (ms); **n_users_retained / n_users_removed:** participants included / excluded; **n_trials_retained / RemovedTrials%:** trials kept and percentage removed; **effect / F / num_df / den_df / p_value / pes:** effect tested, F statistic, numerator and denominator degrees of freedom, p-value, and partial eta squared.

RT Low	RT Upper	n_users retained	n_users removed	n_trials retained	RemovedTrials%	effect	F	num_df	den_df	p	pes
100	20000	42	0	989	2.37	pair	27.22	1	41	<0.001	0.399
100	20000	42	0	989	2.37	presentation_format	29.19	1	41	<0.001	0.416
100	20000	42	0	989	2.37	pair:presentation_format	5.21	1	41	0.028	0.113
100	15000	42	0	969	4.34	pair	26.44	1	41	<0.001	0.392
100	15000	42	0	969	4.34	presentation_format	28.77	1	41	<0.001	0.412
100	15000	42	0	969	4.34	pair:presentation_format	6.36	1	41	0.016	0.134
100	10000	42	0	929	8.29	pair	23.50	1	41	<0.001	0.364
100	10000	42	0	929	8.29	presentation_format	27.52	1	41	<0.001	0.402
100	10000	42	0	929	8.29	pair:presentation_format	7.39	1	41	0.010	0.153
100	8000	42	0	903	10.86	pair	23.12	1	41	<0.001	0.361
100	8000	42	0	903	10.86	presentation_format	27.75	1	41	<0.001	0.404
100	8000	42	0	903	10.86	pair:presentation_format	6.54	1	41	0.014	0.138

7 SUPPLEMENTARY RESULTS: DESCRIPTIVE AND SECONDARY ANALYSES ACROSS EXPERIMENTS

In this section, we report descriptive statistics and secondary inferential analyses for all experiments. All primary analyses are reported in the main text; here, we provide detailed participant-wise summaries and additional exploratory comparisons to support transparency and interpretability.

For each experiment, descriptive statistics include the mean, standard deviation (SD), median, interquartile range (IQR), and 95% confidence intervals (CI) for each dependent variable (accuracy, reaction time, and difficulty ratings), separately for each combination of experimental conditions (e.g., stimulus type \times pair type). The number of participants (N) retained reflects exclusion of low-performing individuals (catch trial accuracy < 0.8) and trials outside the duration cutoffs (< 100 ms or $> 20,000$ ms). These statistics provide an overview of central tendency, variability, and precision of estimates across conditions.

Where applicable, secondary inferential analyses are also reported. These include repeated-measures ANOVAs and post-hoc paired comparisons, conducted to explore patterns not directly addressed in the primary analyses. Significant effects of experimental manipulations are summarized with standard APA-style statistics (F, df, p, partial η^2 or t, df, p, Cohen's d). These supplementary analyses are intended to provide additional context to the main findings and to allow readers to evaluate the robustness and consistency of the observed effects across experiments.

Tables S9–S12 present the descriptive statistics and, where relevant, secondary inferential results, in a structured format for easy reference.

Table S9. Descriptive statistics for Experiment 1 across stimulus and pair types. **Mean / SD / Median / IQR / 95% CI:** participant-wise mean, standard deviation, median, interquartile range, and 95% confidence interval of the dependent variable; **N:** number of participants included.

Stimulus	Pair	Mean Acc	SD Acc	Median Acc	IQR Acc	95% CI Acc	Mean RT	SD RT	Median RT	IQR RT	95% CI RT	Mean Diff	SD Diff	Median Diff	IQR Diff	95% CI Diff	N
rectangle	CD	0.83	0.16	0.91	0.19	[0.79, 0.87]	4353.23	2324.47	3820.75	2813.28	[3769.90, 4936.56]	3.94	0.80	4.00	1.00	[3.74, 4.14]	61
rectangle	TD	0.92	0.12	1.00	0.08	[0.89, 0.95]	3541.06	1883.37	2963.75	1552.67	[3068.42, 4013.69]	3.44	0.83	3.50	1.10	[3.23, 3.65]	61
star	CD	0.70	0.19	0.67	0.27	[0.66, 0.75]	4828.74	2517.94	4477.50	3710.03	[4196.86, 5460.62]	3.91	0.96	3.83	1.47	[3.67, 4.15]	61
star	TD	0.88	0.16	1.00	0.18	[0.84, 0.92]	4641.23	2374.49	4357.25	2887.25	[4045.35, 5237.12]	3.73	0.80	3.91	1.20	[3.53, 3.93]	61

Table S10. Descriptive statistics for Experiment 2 choice percentages and reaction times. Choice percentages are in %, RT is in milliseconds. **CI95:** 95% confidence interval of the mean.

Alternative	Mean	SD	Median	IQR	CI95
Target	51.78	29.46	53.85	48.61	[51.30, 52.26]
Competitor	45.49	30.32	41.18	51.47	[44.99, 45.98]
Decoy	2.73	6.28	0	2.78	[2.63, 2.84]
RT	3942.83	3836.59	2369	3505.5	[3854.53, 4031.13]

Table S11. Descriptive statistics for Experiment 3. Choice percentages are reported in %, reaction times (RT) in milliseconds. **CI95:** 95% confidence interval of the mean.

Alternative	Mean	SD	Median	IQR	CI95
Target (%)	47.62	49.95	0.0	100.0	[46.62, 48.61]
Competitor (%)	48.34	49.98	0.0	100.0	[47.35, 49.34]
Decoy (%)	4.04	19.69	0.0	0.0	[3.65, 4.43]
RT (ms)	2326.76	2273.20	1596.0	1567.0	[2281.46, 2372.05]

Table S12. Experiment 4: Participant-wise descriptive statistics for Accuracy, RT, and Difficulty rating. Accuracy is proportion, RT is in milliseconds, Difficulty rating is on its scale.

Pair	Presentation	Accuracy_Mean	Accuracy_SD	Accuracy_Median	Accuracy_IQR	Accuracy_CI95	RT_Mean	RT_SD	RT_Median	RT_IQR	RT_CI95	Difficulty_Mean	Difficulty_SD	Difficulty_Median	Difficulty_IQR	Difficulty_CI95
CD	aligned	0.85	0.19	0.92	0.19	[0.79, 0.91]	3817.84	2098.70	3290.08	2111.18	[3163.84, 4471.84]	4.09	1.05	4.17	1.17	[3.76, 4.42]
CD	oblique	0.85	0.17	0.83	0.17	[0.80, 0.90]	4240.15	2086.01	3913.83	3105.68	[3590.10, 4890.19]	4.35	0.90	4.42	1.00	[4.07, 4.63]
TD	aligned	0.89	0.21	1.00	0.17	[0.82, 0.95]	2966.74	1527.09	2488.58	1232.88	[2490.86, 3442.61]	3.38	0.96	3.27	1.17	[3.08, 3.68]
TD	oblique	0.85	0.18	0.83	0.17	[0.80, 0.91]	3736.91	1717.62	3627.02	2437.17	[3201.66, 4272.16]	3.94	0.96	3.92	1.29	[3.64, 4.24]

Table S13. Repeated-measures ANOVA results for Experiment 4. Accuracy and RT are reported side by side for each effect.

Effect	Accuracy			RT		
	F(df1, df2)	p	η_p^2	F(df1, df2)	p	η_p^2
pair	1.26(1, 41)	0.269	0.03	9.35(1, 41)	0.004	0.19
presentation	0.8(1, 41)	0.375	0.02	6.69(1, 41)	0.013	0.14
pair:presentation	0.48(1, 41)	0.492	0.01	0.76(1, 41)	0.387	0.02

Table S14. Planned pairwise post-hoc comparisons for Accuracy and RT in Experiment 4. *p*-values are Holm–Bonferroni corrected. Cohen’s d_z and 95% CI are reported.

Contrast	DV	<i>t</i>	df	<i>p</i> _{raw}	<i>p</i> _{holm}	d_z	95% CI
TD aligned vs CD aligned	Accuracy	1.13	41	0.266	0.882	0.17	[-0.13, 0.48]
TD oblique vs CD oblique	Accuracy	0.21	41	0.833	1.000	0.03	[-0.27, 0.34]
TD aligned vs CD oblique	Accuracy	1.24	41	0.220	0.882	0.19	[-0.11, 0.50]
CD aligned vs TD oblique	Accuracy	0.06	41	0.956	1.000	0.01	[-0.29, 0.31]
TD aligned vs CD aligned	RT	-2.88	41	0.006	0.019	-0.44	[-0.76, -0.12]
TD oblique vs CD oblique	RT	-1.68	41	0.101	0.202	-0.26	[-0.56, 0.05]
TD aligned vs CD oblique	RT	-4.04	41	0.00023	0.001	-0.62	[-0.95, -0.29]
CD aligned vs TD oblique	RT	0.25	41	0.804	0.804	0.04	[-0.26, 0.34]

REFERENCES

- Bates, D., Mächler, M., Bolker, B., and Walker, S. (2015). Fitting linear mixed-effects models using lme4. *Journal of statistical software* 67, 1–48
- Farmer, G. D., Warren, P. A., El-Deredy, W., and Howes, A. (2017). The effect of expected value on attraction effect preference reversals. *Journal of Behavioral Decision Making* 30, 785–793
- Spektor, M. S., Kellen, D., and Hotaling, J. M. (2018). When the good looks bad: An experimental exploration of the repulsion effect. *Psychological science* 29, 1309–1320. Publisher: Sage Publications Sage CA: Los Angeles, CA
- Spektor, M. S., Kellen, D., and Klauer, K. C. (2022). The repulsion effect in preferential choice and its relation to perceptual choice. *Cognition* 225, 105164. Publisher: Elsevier
- Trueblood, J. S., Brown, S. D., Heathcote, A., and Busemeyer, J. R. (2013). Not just for consumers: Context effects are fundamental to decision making. *Psychological science* 24, 901–908
- Wedell, D. H. (1991). Distinguishing among models of contextually induced preference reversals. *Journal of Experimental Psychology: Learning, Memory, and Cognition* doi:10.1037/0278-7393.17.4.767